applied sciences

MDPI

Article

MODFLOW Application for Exploitable Groundwater Resource Assessment of the Zhem Artesian Basin Aquifer Complex, Kazakhstan

Daniyar Serikovich Sapargaliyev [1,2], Yermek Zhamshitovich Murtazin [1], Vladimir Mirlas [3], Vladimir Alexandrovich Smolyar [1] and Yaakov Anker [3,4,5,*]

[1] Institute of Hydrogeology and Geoecology Named After U.M. Ahmedsafin, Satbayev University, Almaty 050010, Kazakhstan; rgzgroup1@gmail.com (D.S.S.); ye_murtazin@list.ru (Y.Z.M.); v_smolyar@mail.ru (V.A.S.)
[2] Department of Water, Oil and Gas Resources and Geo-Risks, Kyrgyz State Technical University Named After I. Razzakov, Bishkek 720044, Kyrgyzstan
[3] Department of Chemical Engineering, Ariel University, Ariel 40600, Israel; vladimirm@ariel.ac.il
[4] Department of Environmental Research, Eastern R&D Center, Ariel 40600, Israel
[5] Renewable Energy and Energy Efficiency Group, Department of Infrastructure Engineering, Melbourne School of Engineering, The University of Melbourne, Melbourne, Victoria 3010, Australia
* Correspondence: kobia@ariel.ac.il or yaakov.anker@unimelb.edu.au

Abstract: Groundwater resources are becoming increasingly scarce, especially in arid regions of western Kazakhstan. By 2070, the domestic and drinking water demands will increase from 640 to 901 thousand m^3/day. This deficiency may be overcome by utilizing the Zhem Artesian Basin's Cretaceous Albian–Cenomanian aquifer complex. The hydrodynamic interactions between the 123 known aquifer segments and recharge zones of these promising, exploitable, high-quality groundwater sources are unclear. While MODFLOW is a nominal platform for groundwater flow assessment, which is usually used for the simulation of simple hydrological scenarios, in this study, integrating several different scales and functional modules over a GIS platform enabled delineation and the forecast of this multi-layer aquifer complex. The MODFLOW simulation assessed exploitable groundwater resources and reservoir interactions, enabling the establishment of a simultaneous operation to the Zhem aquifer complex and its neighboring reservoirs. The model suggests that the total exploitable groundwater resources may grow to 629.4 thousand m^3/day during the next 50 years. The simultaneous drawdown model suggests a water level decrease of up to 80 m at the end of this period, which will cause a river flow reduction of approximately 6% of the average long-term river flow. Thus, the assessed exploitable groundwater resources will cover more than 70% of the future regional water demand. The mathematical model developed may be used for monitoring and forecasting groundwater head and water balance changes and may be applied to attain a more detailed groundwater resource transfer scheme with economic criteria.

Keywords: exploitable groundwater resources; numerical modeling; Zhem Artesian Basin; groundwater withdrawal; permissible head drawdown; MODFLOW model

check for updates

Academic Editor: Andrea L. Rizzo

Received: 26 March 2025
Revised: 4 May 2025
Accepted: 5 May 2025
Published: 13 May 2025

Citation: Sapargaliyev, D.S.; Murtazin, Y.Z.; Mirlas, V.; Smolyar, V.A.; Anker, Y. MODFLOW Application for Exploitable Groundwater Resource Assessment of the Zhem Artesian Basin Aquifer Complex, Kazakhstan. *Appl. Sci.* **2025**, *15*, 5443. https://doi.org/10.3390/app15105443

Copyright: © 2025 by the authors. Licensee MDPI, Basel, Switzerland. This article is an open access article distributed under the terms and conditions of the Creative Commons Attribution (CC BY) license (https://creativecommons.org/licenses/by/4.0/).

1. Introduction

Once water demand exceeds availability due to population expansion and development, groundwater becomes a critical freshwater resource, especially in countries under arid conditions with surface water deficits [1,2]. Water obstruction in neighboring regions,

and climate change aggravate water scarcity and freshwater resource depletion [3], while pollution from various anthropogenic sources further deteriorates water resource quality and quantity [4]. During rural area development, land utilization might impair the natural groundwater recharge mostly in terms of quantity reduction and to lesser extent in terms of quality deterioration [5]. In Kazakhstan's arid areas, groundwater resource demand is constantly increasing [6] to a level where half of Kazakhstan's freshwater supply relies on groundwater and the rest on surface flow.

Groundwater resource assessment should consider the basin's geology and hydrogeology, groundwater quantity versus recharge and usage, groundwater quality, and environmental challenges [7]. Groundwater resource assessment using a water balance by groundwater level fluctuation method and base flow hydrograph analysis of the Koyna River Basin, India, supplied a static groundwater reserve assessment and safe exploitable dynamic groundwater reserve potential [8]. During intensive pumping, a significant thickness of the aquifer is drained, and it transitions to an unsaturated state. Under these conditions, subsidence phenomena may occur, especially under seismic impacts [9]. Integrating existing datasets over a geographic information system (GIS) platform enables the delineation of climatic, hydrological, hydrogeological, and environmental features as well as rainfall-runoff modeling. This basic knowledge enables groundwater resource planning for groundwater-dependent ecosystems, such as in the Pilbara region of Western Australia [10].

There are two major types of mathematical models, namely stochastic and deterministic [11,12]. Stochastic models allow for assessing the relations between the statistical characteristics of aquifers and their flow and transport properties. Stochastic approaches rely on treating hydrogeological parameters as a random field and estimating their properties from prior estimates and available state variables (for example, heads and concentration measurements) [13]. The strengths and weaknesses of stochastic approaches in hydrogeology are discussed in [14]. Deterministic models use closed-form mathematical formulas or the solution of a linear system of equations to interpolate data. These models are based on in-depth knowledge of the aquifer's physical processes [15]. Modern deterministic surface and subsurface flow models, such as FEFLOW, can represent river–aquifer exchange accurately, as demonstrated for unconfined aquifer processes in the Papillons catchment of the lower Var valley [16]. Mathematical deterministic computerized groundwater models are a set of equations that describe groundwater flow and water balance in an aquifer. The equations are solved for each node and the groundwater movement from one node to the neighboring node [17]. Numerical groundwater flow models can be used as a forecasting tool for aquifer water management, to test or refine various conceptual models, and to estimate hydraulic parameters; once integrated, they can also be used for water management [18]. Such models can predict how an aquifer might respond to anthropogenic changes, such as changes in pumping schemes and natural conditions, such as a changing climate [19]. MODFLOW is a nominal platform for groundwater flow assessment, which is usually used for the simulation of large-scale phreatic porous media aquifers [20]. The integration of several different scale models and functional modules over a GIS platform to represent spatial and vertical hydrological variations enables the application of MODFLOW for modeling crystalline and karstic aquifer complexes [21]. The advantage of MODFLOW modeling over groundwater filtration analytical calculations is that the model takes into account the modeled object's actual configuration, including its filtration heterogeneity, the wellfields' interaction, and the change in the aquifer transmissivity with head fluctuations during pumping. The latter circumstance is especially important to consider when assessing the potential operational groundwater reserves, since the maximum permissible head drawdowns, as a rule, make up half of the aquifer thickness.

A unified geographic information system of fresh groundwater resources and reserves in Kazakhstan was created in the ArcGIS environment. Data entered into the system were used to calculate various groundwater reservoir characteristics and to create fresh groundwater resource thematic maps [22]. Groundwater resources distribution in Kazakhstan is not uniform, with approximately 37% of groundwater resources being concentrated in the Balkhash-Alakol Basin in southeastern Kazakhstan [23]. Hydrogeological zoning and regional groundwater resource assessment of natural exploitable groundwater resource reserves indicate that as of 2001, 623 groundwater reservoirs were utilized for various purposes, totaling 43,383.5 thousand m^3/day [23,24].

The Zhem Artesian Basin, located in the Aktobe region of western Kazakhstan, is also a significant groundwater resource. According to the Republic of Kazakhstan Groundwater Deposits Cadaster, 131 groundwater reservoirs and sites have been explored within the Zhem Artesian Basin, with operational reserves of 755 thousand m^3/day confined to Albian–Cenomanian strata and, to a lesser extent (8%), to the aquifer complex of Albian–Cenomanian–Quaternary deposits. The bulk (79%) of groundwater reserves is fresh, with mineralization of up to 1 g/L. Reserves with mineralization of 1–3 g/L make up 14%, and according to Kazakh regulations, these reserves are also suitable for domestic and drinking water supply after minimal water treatment. To date, the Zhem Artesian Basin's degree of groundwater resources development has been determined according to the total amount drinking, industrial and agricultural needs, which is approximately 8.6% of the operational reserves [18,25] Other regions in western Kazakhstan, such as Mangistau and Atyrau, have 4.8, 5.2, and 7.4 times less exploitable groundwater reserves, respectively, than the Aktobe region. By 2030, the drinking water demand in the Aktobe region is predicted to double and reach 321,000 m^3/day [25]. This increase is due to the region's population growth and the development of industrial and agricultural areas. Although mineralization reaches 3 g/L, the Cretaceous Albian–Cenomanian aquifer complex is the most promising water source for this growing demand. By 2070, the freshwater supply projected demand in these administrative regions will increase from 640 to 901 thousand m^3/day. According to a reliability assessment, with the known operational groundwater reserves, once all Zhem Artesian Basin aquifers and wellfields are exploited simultaneously, this poses a very real problem. A sustainable operation scheme will allow a realistic assessment of the potential of the available groundwater resources for ensuring a future water supply to the water-deficient regions of western Kazakhstan.

The Zhem Artesian Basin's exploitable groundwater resources consist of several Cretaceous aquifers comprising an aquifer complex. The utilization of the Emba site, located in the northeastern Kokzhide aquifer, started in 2008 after a reassessment (following the initial assessment in 1983). In 2021, the exploitable reserves of the Kokzhide aquifer were re-estimated based on MODFLOW modeling results [26]. MODFLOW models have also been used to determine the exploitable reserves of Kundaktakyrskoye [27], Kandagachskoye [28], Sarybulakskoye [29], and Moiseevskoye [30]. These two- to three-layer models reproduce the hydrogeological conditions of the Quaternary and Albian–Cenomanian Cretaceous aquifer complexes in the vicinity of only these well fields. Since these models were not able to simulate sub-aquifers' interactions within and adjacent to the Zhem Artesian Basin, the entire MODFLOW model of the aquifer complex was developed in this work for the first time.

Thus, the present study aimed to achieve the following goals:

- To assess, via MODFLOW simulation, the present and future exploitable groundwater resources of the Zhem Artesian Basin Cretaceous aquifer complex.
- To develop a groundwater utilization scheme that ensures the future water supply to settlements and industrial facilities in western Kazakhstan.

2. Materials and Methods

2.1. Background and Geographical Framework of the Zhem Artesian Basin

The Zhem Artesian Basin is located in the eastern part of the Caspian depression and is bordered in the northeast by the South Pre-Ural Basin, in the east and south by the Dongystau-Predmugalzharsky Basin, in the southwest by the North Caspian basin, and in the northwest by the Syrtovsky Basin (Figure 1). At 104,000 km^2, the basin's area is administered as follows: 85,000 km^2 or 82% belong to the Aktobe district's northwestern part, 15,000 km^2 or 14% belong to the sparsely populated territory of eastern Atyrau, and 4000 km^2 or 4% belong to the Western Kazakhstan district. Absolute elevations range from 50–75 mAS in the southwest to 300–420 m in the east–northeast. The basin is part of the Ural–Emben plateau, which is dissected by numerous shallow depressions demonstrating a ridged hilly morphology owing to a dense erosion network that is related to the Khobda, Uil, Sagyz, Temir, and Emba river valleys' drainage, combined with remnant table hills and ridges as high as 80–100 m above the valley plateau datum.

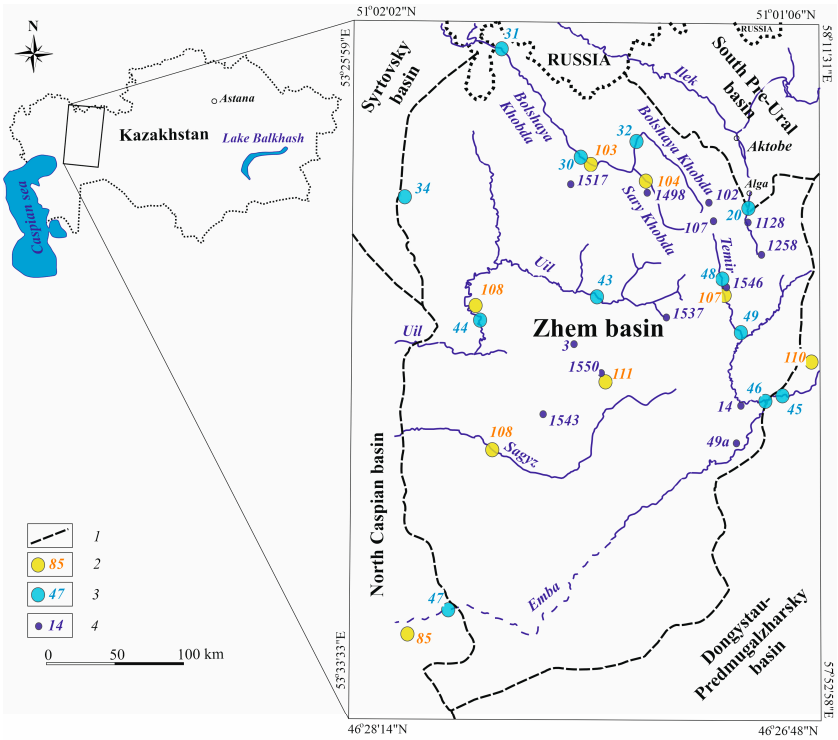


Figure 1. The locations of the Zhem Artesian Basin. 1—basin boundary; 2—meteorological station and its number; 3—hydrological station and its number; 4—observation well and its number.

The mean annual precipitation is 217 mm, with minimum and maximum values of 114 mm and 402 mm, respectively, gradually increasing in the northeast direction. While the Khobda and Emba rivers have natural flow patterns, the rest are disturbed by hydraulic structures (dams). The mean annual flow rate of the rivers varies from 0.5 m^3/s to 6.4 m^3/s, depending on the catchment area and the amount of precipitation.

From a geological and structural composition perspective, the Zhem Basin belongs to the inner bordering part of the Pre-Caspian Depression, which is a deep structure in the vast Russian foundation platform. The Pre-Paleozoic folded foundation depth changes stepwise from 5 to 12 km from the border to the center, covered by a sedimentary cover with four structural stages [24,31]. The most promising Zhem Artesian Basin water supply resource is the sedimentary cover's third structural stage, consisting of Oligocene sandy

argillaceous and Triassic–Carbonaceous sediments with a total thickness of 2–3 km that are confined to stratigraphic and lithologic facial sediment complexes (Figure 2).

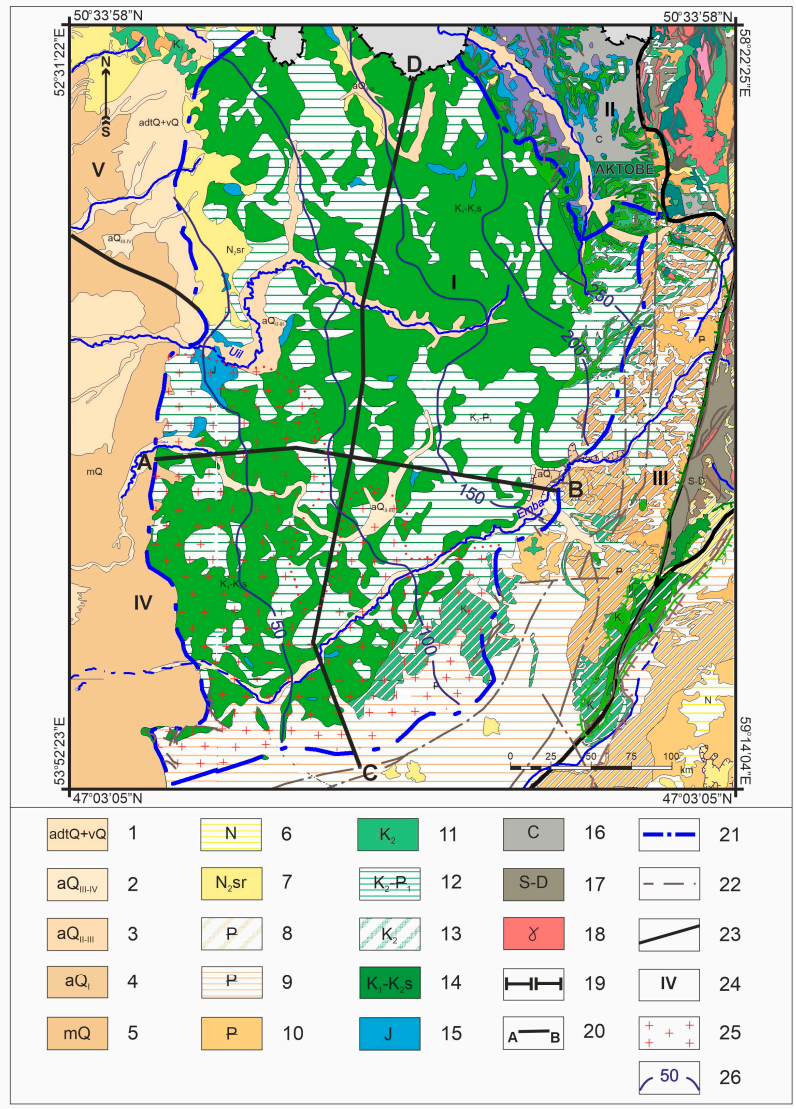


Figure 2. Hydrogeological sketch of the Zhem Artesian Basin. 1—Upper Quaternary alluvial–deltaic and overlying aeolian sediments aquifer; 2—Upper Quaternary–Modern alluvial sediments aquifer; 3—Middle-Upper Quaternary alluvial sediment aquifer; 4—Lower Quaternary alluvial sediment aquifer; 5—Quaternary marine sediment aquifer; 6—Neogene aquiclude; 7—Pliocene Syrt sediment aquifer; 8—local Paleogene aquifer; 9—Paleogene aquiclude; 10—Paleogene clastic sediment aquifer; 11—Upper Cretaceous aquifer; 12—Upper Cretaceous and Paleogene aquiclude; 13—local Upper Cretaceous aquifers; 14—Lower Cretaceous–Cenomanian sediment aquifer complex; 15—Jurassic aquifer complex; 16—carboniferous aquifer of fractured coal rocks; 17—Silurian–Devonian aquifer; 18—Magmatic aquifers; 19—Kazakhstan border; 20—hydrogeological cross-section line; 21—Zhem Basin boundary; 22—rifts; 23— basin divide lines; 24—Artesian basins: I—Zhem Basin; II—South Pre-Ural Basin; III—Dongystau-Predmugalzharsky Basin; IV—North Caspian Basin; V—Syrtovsky Basin; 25—brackish and saline groundwater recharge area 3–10 g/L; 26—natural groundwater head.

The hydrogeological cross-section of the Zhem Artesian Basin exploitable aquifer complex (Figure 3) consists of the following sections.

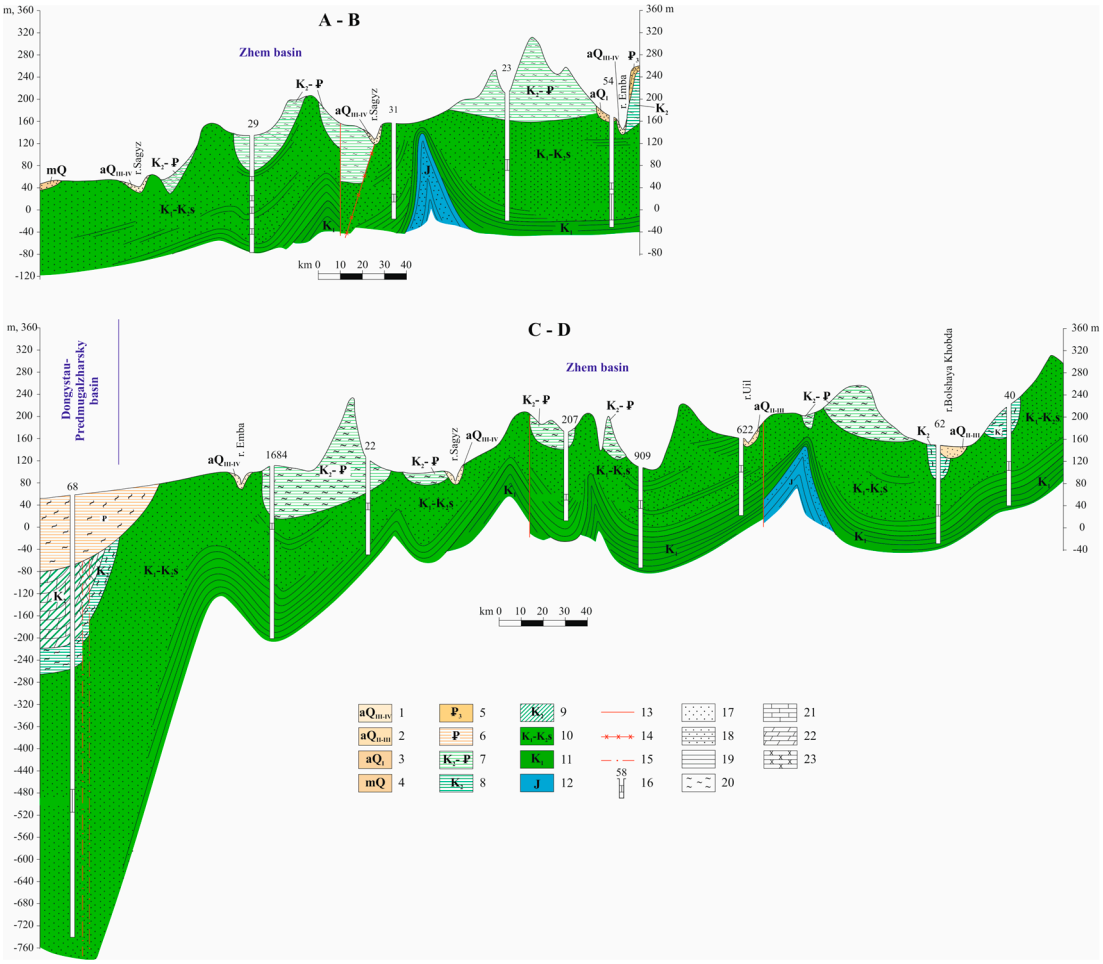


Figure 3. Hydrogeological cross-sections along the A–B and C–D lines (in Figure 2). 1—Upper Quaternary–Modern alluvial aquifer; 2—Middle–Upper quaternary alluvial aquifer; 3—Lower Quaternary alluvial aquifer; 4—Quaternary marine sediment aquifer; 5—local Paleogene deposit aquifer; 6—impermeable Paleogene sediments; 7—Upper Cretaceous and Paleogene aquiclude; 8—Upper Cretaceous aquiclude; 9—local Upper Cretaceous aquifer; 10—Lower Cretaceous–Cenomanian aquifer complex; 11—Lower Cretaceous aquifer complex; 12—Jurassic aquifer complex; 13—hydrogeological unstudied fault; 14—water-bearing fault; 15—fault hidden under overlying strata and inferred from geophysical data; 16—Borehole with sampling interval; the borehole number is at the top. Lithology: 17—sands; 18—clayey sands; 19—clays; 20—impermeable horizon clays; 21—chalk; 22—marls; 23—sandstones.

Upper Quaternary to Modern (aQ_{III-V}) and Middle–Upper Quaternary (aQ_{II-III}) alluvial sediment aquifers are located in the river valleys and confined to the alluvial deposits of floodplains. The first and second terraces above the floodplain are represented by heterogeneous, sometimes gravelly sands interbedded with light loams and clay. The aquifer thickness varies from 5 to 18 m, and in some deep valley sections, it reaches 50–60 m (Ilek River valley). The aquifer hydraulic conductivity ranges from 1 to 12 m/day, with depths of up to 5 m in the floodplain and the first terrace above the floodplain, and 12–15 m in higher terraces. The pumping well flow rates vary from 1 to 2.5 L/s, with the total salinity of groundwater increasing downstream from 0.8 to 3.0 g/L.

The Lower Quaternary alluvial deposit (aQI) aquifer is confined to the third floodplain terrace and geographically coincides with the Kokzhide and Kumzhargan aeolian sand boundaries. Groundwater is confined to heterogeneous sands with lenses of gravel, with an aquifer thickness that reaches 11 m or more. Depending on the hypsometry of the surface,

the groundwater table depth varies from 2.2 to 28.9 m. The pumping well flow rates range from 1 to 13 L/s. The total salinity of the groundwater is 0.1–0.2 g/L.

The local Paleogene aquifer and aquiclude (P) have a limited distribution in the eastern and southern Zhem Basin parts in the form of watershed surface remnants. The thickness of the water-bearing sands and sandstones rarely exceeds 3–5 m, with an interlayered unit total thickness of 10–15 m and a pumping flow rate of 0.025–1 L/s. The semi-confined groundwater is at a 5–16 m depth. The groundwater is fresh to slightly brackish, with a total salinity of 0.8–5 g/L. The impermeable layers are Tripoli- and Opoka-like clays with interlaying sands and weakly cemented sandstones, with a total thickness of up to 50 m.

Upper Cretaceous Campanian to Lower Paleogene regional aquitards (K2-P and K2) underlie the watershed areas, with a thickness that varies from 10 m to 90 m. This aquitard stratum restricts the discharge from the Albian aquifer complex. The local Upper Cretaceous aquifer (K2) has a limited distribution and is composed of sandy marls and clays with a total thickness of up to 40 m. The lower Cretaceous–Cenomanian aquifer complex (K1-K2s) is the most promising and widespread in the Zhem Basin. In places across the basin, the aquifer complex groundwater reaches the surface or is covered by thin alluvial sediments. Clay and marl sediment cover the aquitard, confining the Upper Cretaceous sandstone aquifer vertically and spatially. The sediment thickness varies from 25 to 980 m and is 147 m on average. The groundwater heads range from 4 to 383 m above the complex datum and are 49 m on average. Filtration coefficients vary from 0.8 to 29.8 m/day, and the pumping rates range from 6 to 40–63 L/s. The total salinity of groundwater ranges from 0.2 to 5.3 g/L, with a general increase from the northeast to the southwest in the groundwater flow direction.

The lower Cretaceous Aptian–Neocomian aquifer complex (K1) lies at a depth of 90 to 1100 m with a 30 to 100 m thickness range. It is comprised of sands interlaced with pebbles and clay layers. The clay cover separates it from the overlying lower Cretaceous–Cenomanian complex. The Jurassic aquifer (J) is exposed in restricted areas between salt domes, while in other areas, it occurs at great depths.

2.2. Modeling Setup

2.2.1. Dataset

The modeling dataset includes the following data:

- Fieldwork results, including hydrogeological parameters after assessment and reassessment of exploitable groundwater resources for 77 Albian–Cenomanian aquifer sections;
- Groundwater monitoring data for 2007–2022, collected and analyzed at 13 Kazakh State groundwater monitoring observation posts, characterizing the Albian–Cenomanian aquifer complex. These 13 posts include 54 hydrogeological monitoring wells, from which 13 representative wells were selected and characterized for their maximal groundwater level fluctuation amplitude.
- The Zhem Basin's 2007 to 2022 annual surface water flow rates and water levels were measured at 12 river gauging stations of the Kazhydromet National Hydrometeorological Service.
- Long-term average precipitation data were taken for eight meteorological stations from the "Kazhydromet" meteorological database (https://www.kazhydromet.kz/ru, accessed on 20 April 2025).

2.2.2. The Site Mathematical Computer Modeling Structure

The conceptual approach to model development for this study is shown in Figure 4.

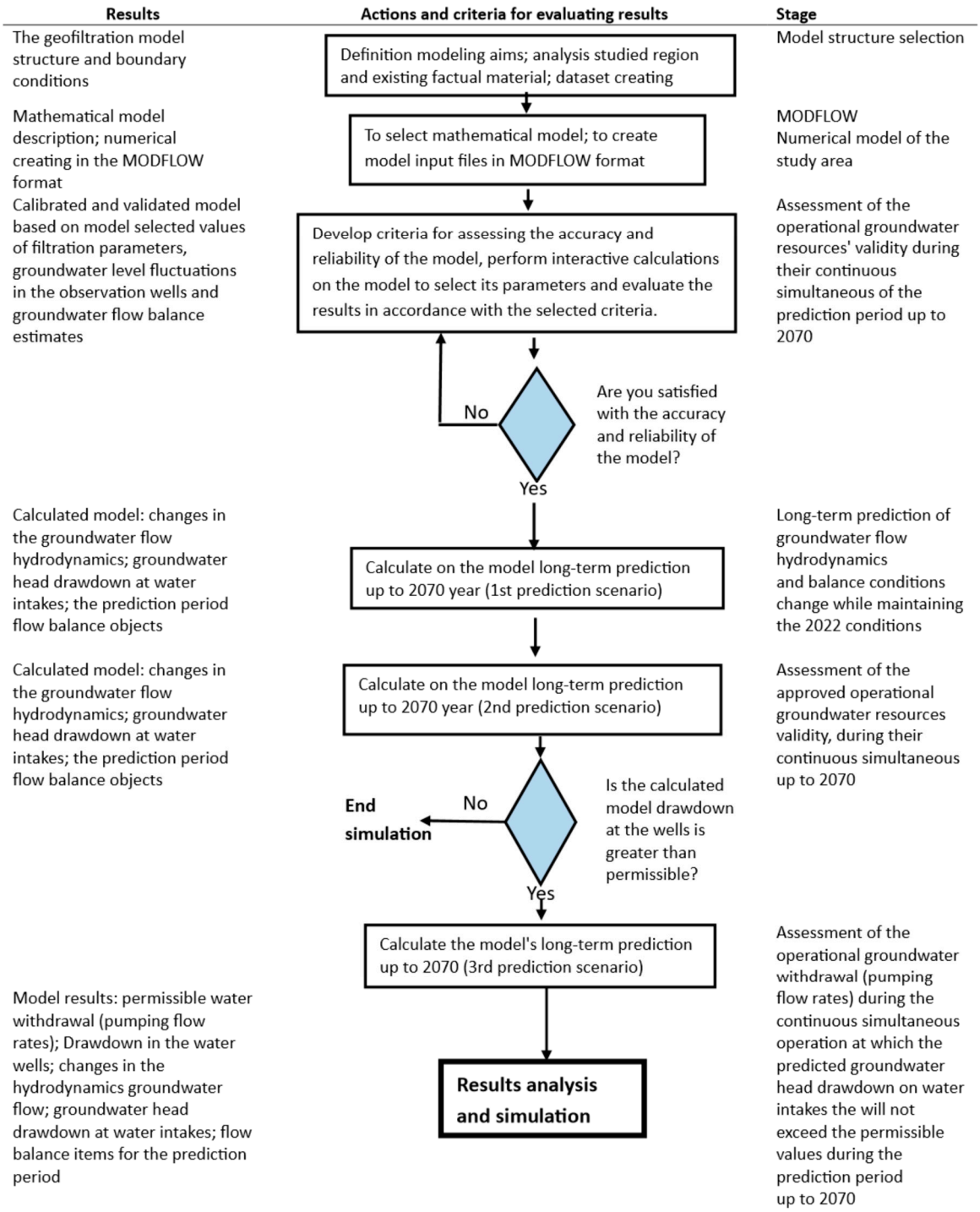


Figure 4. The Zhem Artesian Basin conceptual model development working process.

The mathematical model structure is determined with consideration of the following factors: the modeled object's nominal hydrogeological conditions, which are modeled so that the model content corresponds to the natural object; the possibility of constructing a model that allows solving the tasks with the required accuracy; maintaining option of adjusting the model and introducing various amendments to it during the modeling process; performing modeling while maintaining the specified accuracy of the solution in the most straightforward ways and within adequate timeframes is considered. The groundwater flow structure simplification is carried out by reducing spatial filtration to a simpler one, for example, by reducing the flow dimensions. The Zhem Artesian

Basin model area significant dimensions in terms of the aquifer thickness, almost always make it possible to switch from spatial filtration to a planned filtration. The basin's aquifers are hydraulically interconnected and form a single geofiltration flow, which has a common piezometric surface. The inconsistent clayey layer between the Albian sandy formations and Cenomanian strata suggests a single aquifer complex. (Figure 2). It should be noted that there is insufficient factual material that would allow the modeling of the filtration heterogeneity of the sub-aquifers and the dynamics of the changes in the groundwater heads along the vertical section of the aquifers. This unique definition of these predetermined factors enabled a single-layer creation for the two-dimensional model of the Zhem Artesian Basin Middle–Upper Albian, Cenomanian, and Quaternary aquifer complex. The mathematical model represents groundwater flow through porous media using a two-dimensional partial differential equation for a one-layer geofiltration to an unconfined or confined aquifer. The undifferentiated Middle–Upper Albian and partly Cenomanian Cretaceous sediments and Quaternary sediments are unconfined conditions represented by flow Equation (1) [32], as follows:

$$\partial/\partial x[Kx(Hx - \eta x)(\partial H/\partial x)] + \partial/\partial y[Ky(Hy - \eta y)(\partial H/\partial y)] \pm W = Sy(\partial H/\partial t), \quad (1)$$

where Kx and Ky are the hydraulic conductivity along the principal permeability directions of the x- and y-coordinate axes, respectively; H is the potentiometric head; x and y are the unconfined aquifer floor elevations along the x- and y-coordinate axes; W indicates the fluxes representing recharge, evaporation, and water pumping; Sy is the porous material specific yield; and t is time. For confined conditions, $(Hx - \eta x)$ and $(Hy - \eta y)$ are replaced by mx and my, and Sy is replaced by Ss, where m is the thickness of the aquifer and Ss is the specific storage.

The visual MODFLOW version 4.12 software package [33] (https://www.pdfdrive.com/visual-modflow-20111-users-manual-d22572407.html, accessed on 20 April 2025) [27] was selected for the study because of its ability to calculate flow fluxes across cell boundaries and predict groundwater spatial and temporal head-level distribution [34]. The transformation from unconfined flow to confined conditions and vice versa is automatic with differential calculations of the surface elevation and the calculated groundwater level at each time step. The model boundary conditions are represented as head and flow and their combination. Equation (1) mathematically represents the study area's groundwater flow model. For spatial variability representation, the study area was overlaid with a grid, where each cell is denoted by a point in its center.

2.2.3. Numerical Model Illustration

Once a mathematical conceptual model was established, a computer model consisting of one horizontal layer was built. The model's bottom boundary was the Aptian Lower Cretaceous dense clay top, which was taken as an impermeable boundary. The Albian aquifer complex is comprised of quartz–glauconite sands of varying sizes down to clayey and mainly sandy, sandy loam, sand–gravel–pebble deposits with loam interlayers, clay, and siltstone. The computer model follows the groundwater flow hydraulic gradient from the basin's higher boundaries to the Caspian Basin outlet (Figure 1) that were set as constant flow rates. The basin (Figure 5) and model area dimensions are 510 km in the northern direction and 320 km in the western direction, with a total modeled area of 163,200 km^2. The rectangle's lower left corner is the model coordinates' reference point (X = 0; Y = 0), which corresponds to the geographical coordinates of 46° 28′ 42.48″ N latitude and 53° 49′ 26.76″ E longitude. The model region was divided into a rectangular grid with 64 × 102 computational cells. The grid steps along the axes are uniform and are set equal to 5 km by 5 km. Thus, the area of the computing unit was 25 km^2. The total area of the Zhem Artesian

Basin is 104,000 km^2; the area of the computational block of the model (25 km^2) is 0.02% in relation to the total area of the modeled object. In addition, the linear dimensions of the groundwater extraction area that reach 26.5 km (Kokzhide wellfield) and the distances between the explored well fields exceed tens of kilometers. Taking into account these circumstances, as well as the hydrogeological study of the territory and the insignificant number of observation wells characterizing the long-term regime of groundwater, this computational grid adopted in the modeling meets the accuracy requirements for the problems being solved.

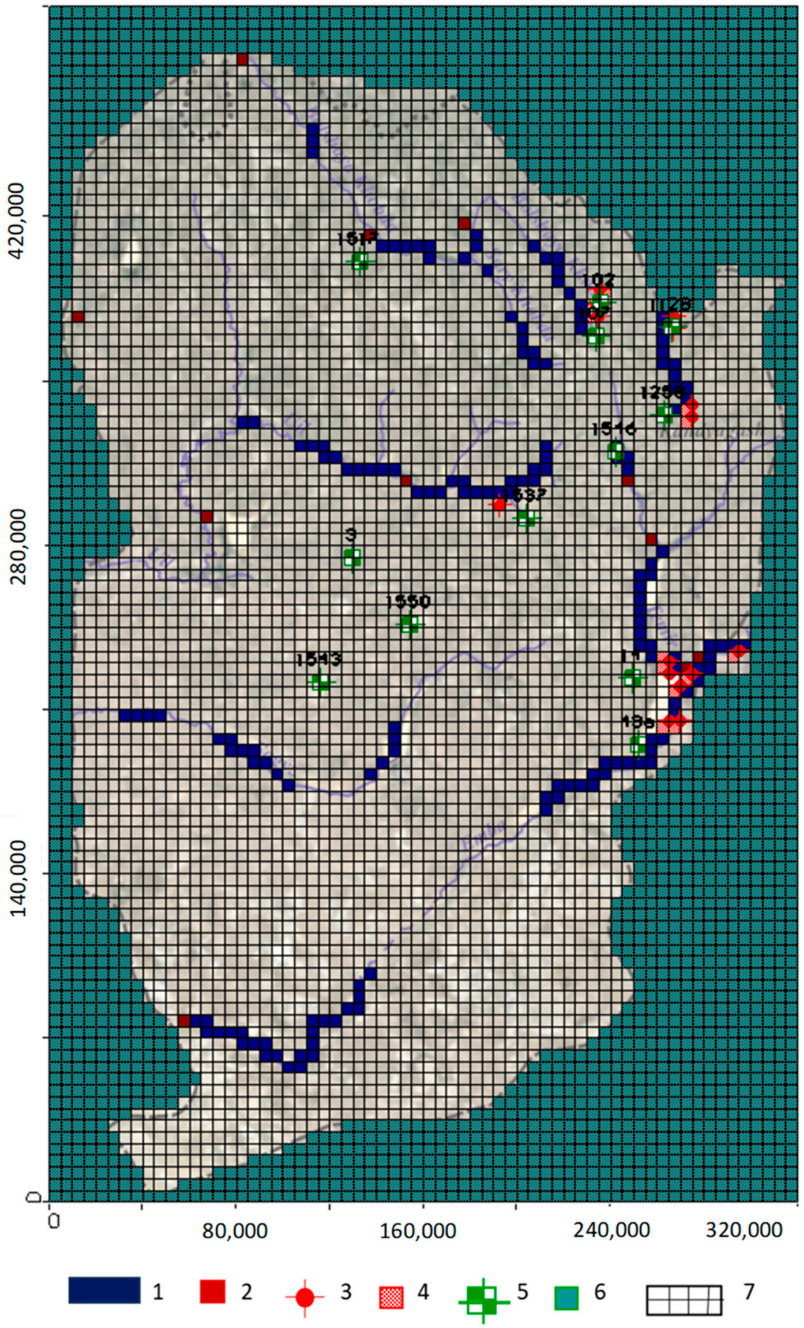


Figure 5. The Zhem Basin model area: model grid and boundary conditions. 1 = river boundary conditions active cells; 2 = constant head boundary conditions; 3 = pumping well; 4 = model cells corresponding to the well location at the aquifer segment; 5 = observation well; 6 = inactive cells (no flow within the model domain); 7 = model grid.

The following boundary conditions were specified in the model:

- The relationships between water levels in the river and groundwater that reflect groundwater recharge/discharge to/from the main rivers flowing through the Zhem Basin, namely Emba, Sagyz, Uil, Temir, and Khobda;
- Groundwater recharge from annual rainfall percolation from the soil surface;
- Mean annual evapotranspiration;
- Total annual groundwater extraction and outlet by aquifers and singular pumping sites.

The groundwater discharge/recharge to/from the primary source is referred to as the boundary condition (BC) of the third kind, i.e., "River" (BC-III), in accordance with the "Visual MODFLOW Pro" version 4.12 software package requirements. These boundary conditions simulate groundwater discharge or recharge from or into the river in areas with a hydraulic connection connection between the river and the aquifer. The flow rate of water entering the aquifer from the river (recharge) or from the aquifer (discharge) was calculated based on the elevation difference given by the groundwater level model. This difference was set as the differential between the water level under the riverbed and the river flow elevation at a given boundary point. If the groundwater level is above this point, groundwater discharges into the river, and below, the runoff recharges the groundwater. Where the riverbed is underlaid by low-permeability, thick sediments that prevent hydraulic interconnection with groundwater, these boundary conditions were not applied. To ensure the model's computational process convergence, constant head boundary conditions (BC-I) were set at the hydrological post locations along the rivers, simulating a direct hydraulic relationship between the surface water and groundwater. Flow rates along these boundaries were calculated during the groundwater flow balance component calculation and were considered the groundwater recharge/discharge rates to/from the river.

Annual rainfall percolation to groundwater was defined as recharge distributed over an area (mm). Considering the area's groundwater depth and relatively high summer temperatures, the initial value of areal recharge was set at 10% of the total annual atmospheric precipitation and was subsequently adjusted during model identification.

The model's evapotranspiration (ET) BC was set to the entire model area, given that the evapotranspiration potential and the groundwater relationship were set as linear. Since MODFLOW is not functionally designed to calculate vadose (unsaturated) zone water flow, the evapotranspiration value calculated in the model reflects the flow rate coming from the groundwater level surface into the unsaturated zone without considering its direct movement. Evapotranspiration was calculated for each time step, depending on the groundwater level depth and the potential surface evapotranspiration corresponding to open water surface evaporation. Evapotranspiration decreases with groundwater level depth, up to a critical groundwater evapotranspiration (Hcr) depth of 3.0 m where the evapotranspiration value becomes negligibly small, which is dictated by the unsaturated zone prevailing lithological composition. In accordance with the State Commission for Mineral Reserves of the Republic of Kazakhstan (GKZ RK) [27,29], a long-term average water surface evaporation of 900 mm/year was set, which reflects the central part of western Kazakhstan [24,27,29].

The annual groundwater pumping for a specific post was quantified using the "Pumping well" MODFLOW tool for model cells representing a given aquifer segment or single water well. The pumping rates changed yearly according to the annual values from 2007 to 2022. The model time step was specified in days from the beginning of the model calculation (start time—0 days = 1 January 2007). Intermediate time steps were set automatically depending on the boundary conditions, time of change, and observation periods (stress periods) within a calculation period. Since the stress periods for the model were specified in average annual values, the calculation results were written to the model output file with

a timestep of one year. The total model calculation duration was 23,000 days (to 2070), which is the forecast prediction range.

2.2.4. Model Calibration and Validation

The model was run from 1 January 2007 to 31 December 2022 (5475 days), during which the actual system behavior was observed. Wherever the simulated water level and pressure did not match the observed ones, manual adjustments were made to the model's hydraulic conductivity and recharge values assigned to specific layers to characterize the relevant cells. Model calibration continued until a close match between simulated and observed behaviors was achieved by refining the coefficients for layer hydraulic conductivity, aquifer storage, recharge, and water balance. Considering that the observed groundwater head elevation range was 150 m and annual groundwater head fluctuations were 2.5–3.5 m on average, the model's acceptable calibration accuracy in terms of water levels was defined as 1.0 m, and in terms of the groundwater budget, it was defined as 5%. Justification and validation of the calibrated model were based on coincidence, spatial variation in the model region values of the geofiltration parameters obtained from field data measurements and put in the model, within the limits of their geological reliability (usually $\pm$ 50%). The coincidence of water balance elements within the limits of their hydrogeological and hydrological reliability was also estimated.

2.2.5. Model Predictions

The calibrated model was applied to simulate and predict the following three scenarios:

- First (initial) prediction scenario. Long-term prediction of changes in groundwater flow, hydrodynamic, and balance conditions and their resources while maintaining the 2022 prevailing conditions;
- Second prediction scenario. Assessment of the Zhem Basin's approved exploitable groundwater resource security (availability). The second prediction scenario was aimed at checking the availability of approved operational groundwater resources per aquifer and water well in the event of their simultaneous operation. Estimation of exploitable resources, in accordance with the existing approved methodology in Kazakhstan, comes down to comparing the calculated groundwater levels drawdown with water withdrawal equal to the approved resource and the maximum permissible drawdown for a given water well. The calculated drawdown must be less than the maximum permissible drawdown. The maximum permissible drawdown is determined based on the pump's technical capabilities, but must not exceed half the thickness of the pumped aquifer;
- Third prediction scenario. Evaluation of the maximal possible water withdrawal at which the predicted groundwater head drawdown will not exceed the permissible values. This calculation was carried out only for aquifers for which the predicted drawdown of the second scenario exceeded the maximum permissible drawdown.

Predictions were performed for two periods, namely 25 years and 50 years. The beginning of the prediction model corresponded to the end of the calibration model period on 31 December 2022 (5475 days) and ended at 23,000 days. The first prediction scenario evaluated the annual exploitable groundwater withdrawal value for various posts using the 2022 initial parameters. The second prediction scenario assessed the annual groundwater withdrawal-approved exploitable groundwater resource values for 123 aquifer segments. In the third prediction scenario, groundwater withdrawal was the same as in the second scenario, excluding those segments for which the maximum possible water withdrawal was calculated. In all the scenarios, the BCs remained the same as those in 2022.

The Theis solution [35] was used to adjust the model cell size to the average radius of the reservoir (pumping) area, enabling the computation of cell area transition cuts (corrections) of the real well size and modeling to compare the actual drawdowns.

2.2.6. Development of the Numerical Model and Parameter Setting

The Theissen polygon method with the meteorological stations' locations (Figure 6) was applied for the precipitation recharge zone delineation (Table 1) [36,37].

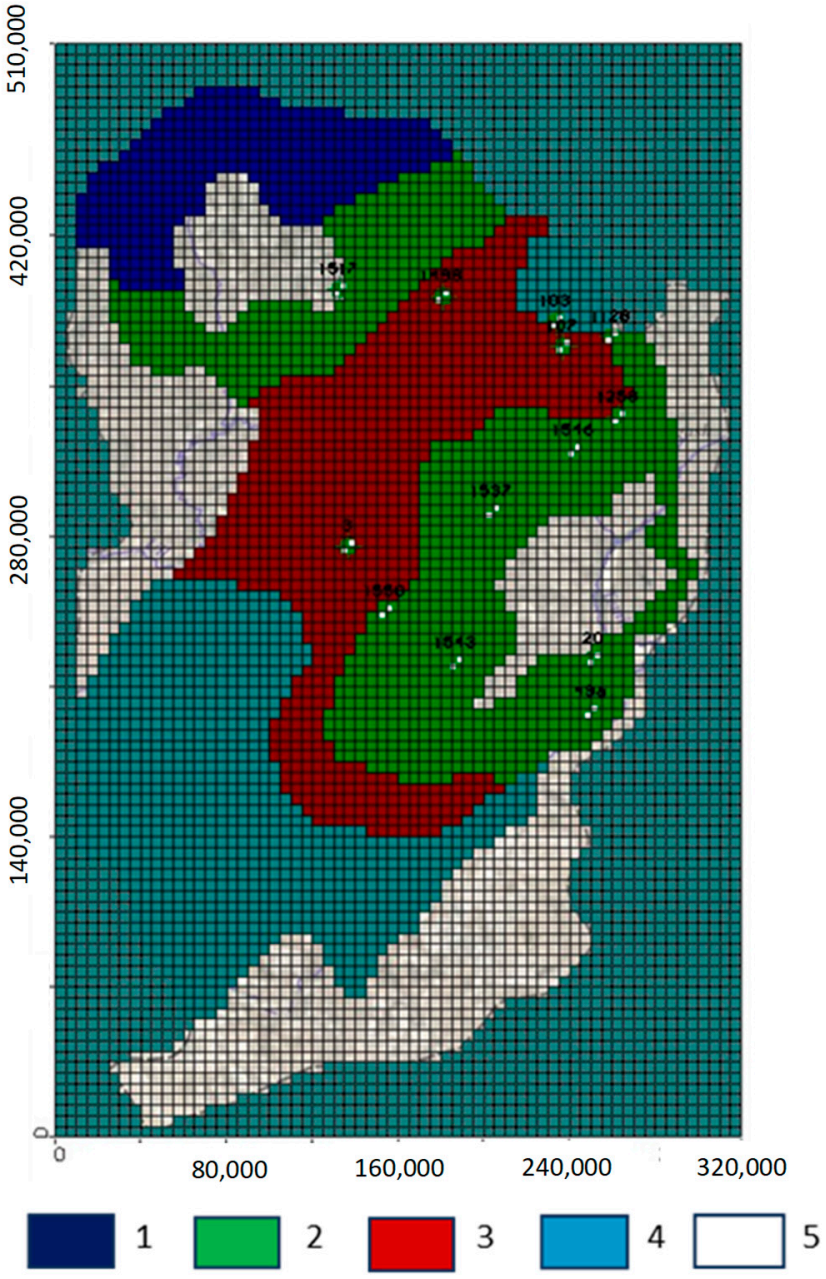


Figure 6. Initial values of annual recharge set in the model recharge zones. 1—29 mm (Theissen polygon number 103); 2—33 mm (104, 108); 3—31 mm (107, 11); 4—22 mm (81, 85, 110); 5—areas where the aquifer is covered by clay sediments, preventing precipitation percolation.

Table 1. Initial values of annual recharge as set in the model, mm.

Post number and the Thiessen polygon number, respectively	103	104	107	108	110	111	81	85
Name of the station	Novoalekseevka (Khobda)	Ilyinsky	Temir	Uil	Emba	Karauylkeldi	Sagyz	Kulsary
Location, river valley	Khobda	Khobda	Temir	Uil	Emba	Watershed	Sagyz	Emba
X-axis coordinate in model, m	138,400	186,800	245,100	66,500	311,500	1,534,000	80,000	11,400
Y-axis coordinate in model, m	410,300	389,100	296,000	291,600	265,000	244,300	193,000	55,600
Post absolute elevation, m	142	190	234	102	251.8	227.2	55.2	−9.1
2007	29	34	32	35	21	29	24	20
2008	25	26	21	24	22	22	22	16
2009	23	21	31	23	27	28	22	14
2010	16	14	15	16	18	16	14	14
2011	30	23	23	40	21	25	18	13
2012	13	12	14	19	15	13	7	13
2013	28	29	32	27	25	32	21	17
2014	15	16	29	24	18	24	15	10
2015	25	16	26	19	24	27	17	16
2016	49	32	47	40	36	48	36	33
2017	21	14	26	23	31	29	20	14
2018	22	18	15	16	12	13	15	6
2019	18	14	15	17	16	18	13	18
2020	24	21	16	17	20	20	15	11
2021	27	17	22	25	17	23	14	5
2022	39	21	24	33	21	23	17	18

The initial hydraulic conductivity (*Kf*) and storage coefficient (*Sy*) values were based on field pumping tests carried out during hydrogeological exploration at the 88 sites. The hydraulic conductivity and storage coefficient for the specified zones were isotropic. Thus, the model's homogeneous groundwater flow representation may be applied for each computational block. The initial *Kf* values were averaged for an entire model layer thickness and calculated as the pumping aquifer effective thickness *Kf* values (Table 2).

Table 2. Conductivity and storage parameters of Cretaceous sediments in the Zhem Basin.

Parameter	Unit	Tested Aquifers and Site Number	Parameter's Value		
			Min	Max	Average
Hydraulic conductivity	m/day	74	0.8	14.1	5.6
Effective thickness	m	76	4	200	43.1
Transmissivity	m^2/day	15	111	1070	490
Specific yield	Dimensionless	45	0.01	0.2	0.13
Specific storage	Dimensionless	36	1×10^{-5}	6×10^{-2}	8.7×10^{-3}

Annual groundwater withdrawal values for the 2007 to 2022 period were evaluated for the Emba, Kenkiyak, Atzhaksy, Alibekmola, Kundaktyr, Kandagach, Alga, Ashikol, and Shubarkuduk areas (Figure 7). Whenever the linear dimensions exceeded the model block size, the water intake was set as equal to several neighboring blocks.

Most groundwater reservoirs (more than 75%) had an uptake of up to 1000 m^3/day for a single well (rural settlements). Groundwater reservoirs with exploitable groundwater resources vary from 1000 to 50,000 m^3/day for the water supplies of district centers and small towns, such as Aktobe and Kandyagash. The water is used for drinking and industrial supply for large commercial areas, such as the technical water supply for oil fields. The largest groundwater reservoir is Kokzhide, with exploitable groundwater resources of 173,400 m^3/day. For groundwater withdrawal above 1000 m^3/day, a linear water extraction scheme that includes several pumping wells (up to 35) was used. The total groundwater withdrawal for the second prediction scenario was 715.500 m^3/day.

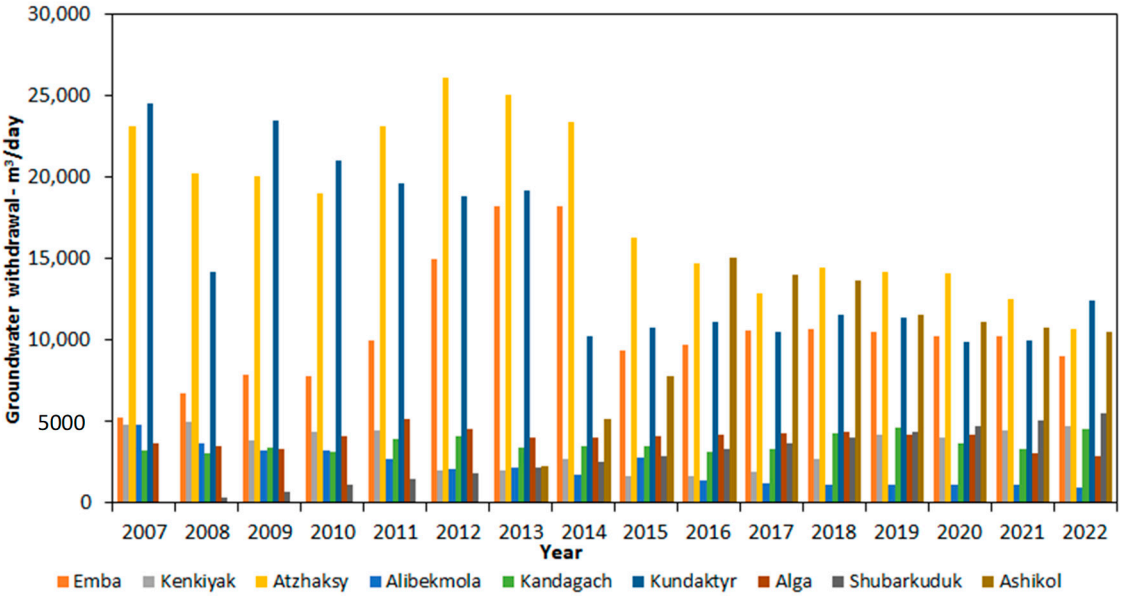


Figure 7. Groundwater withdrawal during 2007—2022 for the various study regions. The locations of the 123 water wells specified in the second and third model prediction scenarios are shown in Figure 8 are aligned to their colors in Figure 7.

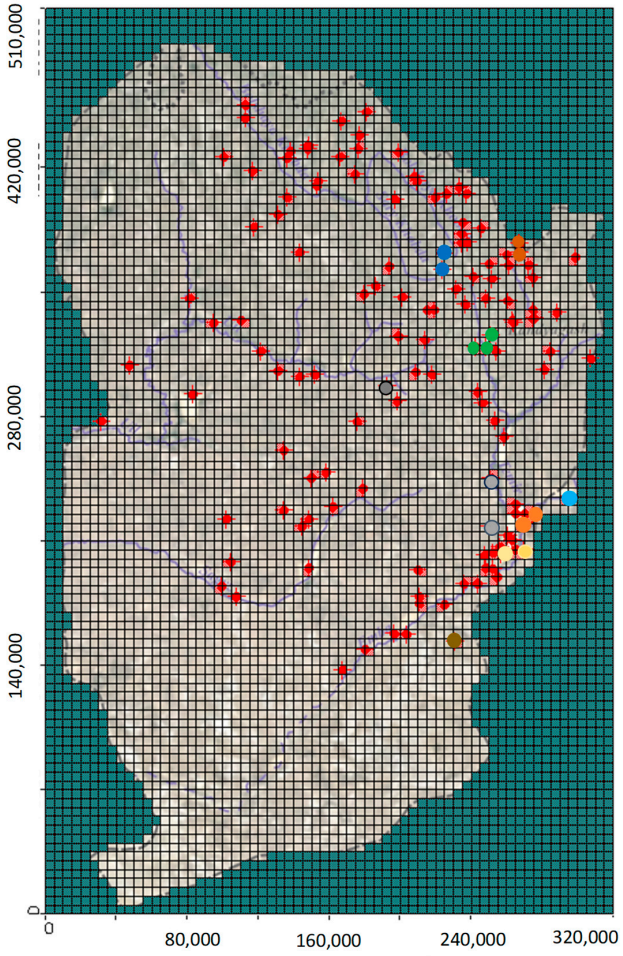


Figure 8. The model's water withdrawal location points (with those for the second and third model prediction scenarios in red).

3. Results and Discussion

While water quantity and quality control groundwater supply demand, almost all aquifers are within the freshwater distribution area, making them attractive water resources. The Zhem Artesian Basin groundwater chemical content of the Lower Cretaceous–Cenomanian aquifer complex's main exploitable segments is illustrated in Figures 9 and 10. The chemical data depicted in the Piper diagram [38] reveal various groundwater types, including Na-K-Cl, Ca-Cl, Ca-Mg-HCO3, mixite Ca-Na-Mg-HCO3, and mixite Ca-Na-Cl (Figure 9). Durov's diagram [39] reflects the correlation between different anions and cation concentrations, pH values, and TDS (Figure 10). As noted in other arid regions [40], fresh and ultra-fresh groundwater has a hydrocarbonate–calcium–magnesium composition, as found at the Kundaktakyrskoye, Kandagachskoye, Sarybulakskoye, and other reservoirs mostly around the Zhem Artesian Basin's northeastern area. Towards the southwest, more saline groundwaters have a chloride–sulphate and sulphate–chloride–hydrocarbonate sodium and sodium–calcium composition. Groundwater chemical analysis results of samples taken from exploration and production wells in various areas of the artesian basin are given in Appendix A and the Republic of Kazakhstan SP-26 drinking water requirements are given in Appendix B, indicating their potential use for the domestic and drinking water supply. Brackish waters with TDS values from 1000 to 3000 mg/L are mainly intended for irrigation. Salty and hard waters exceeding the Kazakh drinking water quality standards can be used only after preliminary quality improvement.

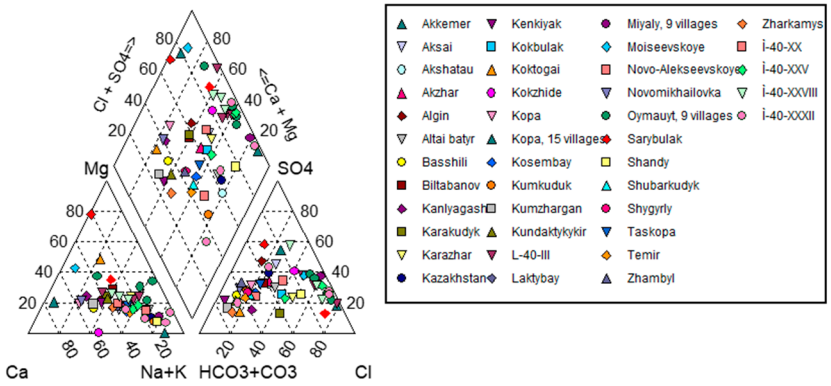


Figure 9. Piper plot depicting groundwater chemical compositions of the Lower Cretaceous–Cenomanian exploitable sites of the Zhem Artesian Basin for the main macro-components.

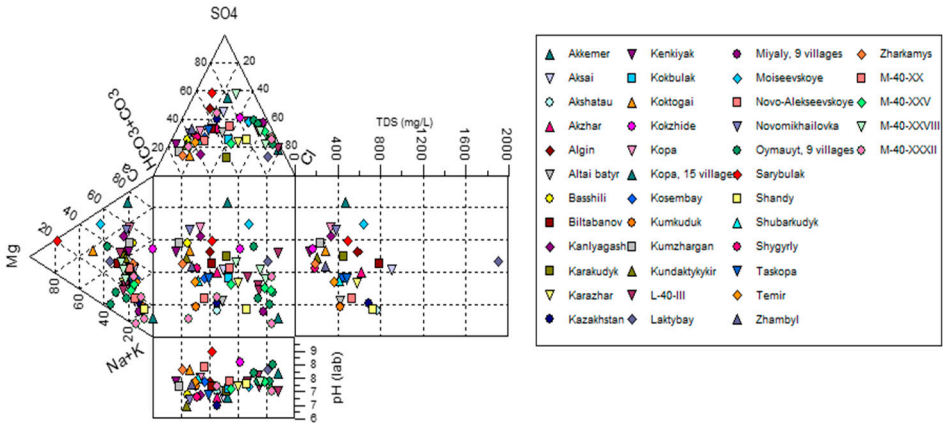


Figure 10. Durov diagram depicting groundwater chemical compositions of the Lower Cretaceous–Cenomanian exploitable sites of the Zhem Artesian Basin.

3.1. Model Calibration and Validation

The sensitivity to changes in various parameters was checked during the first model calibration stage. It was found that changes in the hydraulic conductivity and storage parameter values within the first order do not affect the calculated groundwater levels. With that said, changes in groundwater spatial recharge had a significant impact, confirming the conceptual basin's hydrogeological groundwater formation regime. Thus, the main parameter affecting the model calibration was total groundwater recharge due to atmospheric precipitation infiltration [41].

The model calibration results compare the annual average groundwater level measured values in the observation wells and those calculated by the model with the statistical assessment comparison results (Figures 11 and 12). The residual mean was −0.219 m, the absolute residual mean was 1.24 m, the estimated standard error was 0.44 m, and the root mean square (RMS) was 1.35 m. In addition, the correlation coefficient between the measured and modeled groundwater levels was 1.0 (Figure 11).

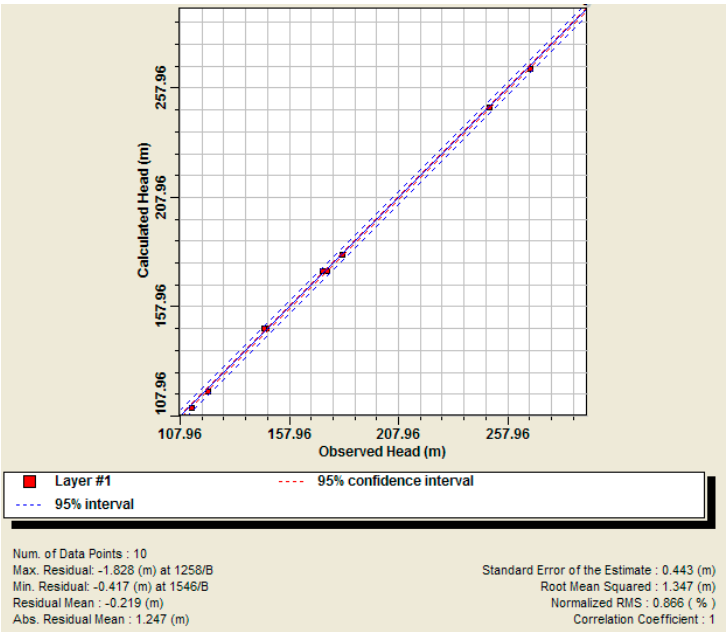


Figure 11. Comparison between a single-layer model-calculated and measured average groundwater levels in the observation wells.

The variance between the measured and the model-calculated groundwater level fluctuations for observation wells with a complete set of observations of average annual values of groundwater head is less than 1 m (Figure 12), with similar results obtained for the remaining observation wells used for model calibration. While these discrepancies can be as high as 30%, they are valid for practical use and within the expected range reported in the literature for Kazakhstan [42]. The statistical assessment of the inverse transient flow problem solution for 2007–2022 accuracy is presented in Table 3.

On average, R^2 was 0.28 m, MAD was 0.35 m, MAE was −0.16, m and RMSE was 0.52 m. The average variance between observed groundwater heads and calculated model heads was 0.21 m. The aquifer's calibrated hydraulic conductivity ranged from 0.7 to 8 m/day (Figure 12), which was in good agreement with the values obtained from field studies and experimental well pumping (Table 2). The differences between hydraulic conductivity values obtained from pumping tests (Appendix C) and the model (Figure 13) vary within ±16–42%, with a given accuracy of the model solutions relative to the hydraulic conductivity values within ±50%, which confirms its hydrogeological reliability. The given

solution accuracy is affected by errors related to the aquifer conceptual model, as well as when switching from calculating the hydraulic conductivity based on the results of experimental pumping within the tested interval at a local point to its average weighted value for the modeled layer thickness. The adjustments that were made to the model's hydraulic conductivity during model calibration showed that an order of magnitude change in this parameter does not affect the calculated groundwater head, which is in good agreement with previous modeling experiments [21–24]. The model calculated the groundwater flow balance ratio (Table 4), which relate to recharge in the input and evapotranspiration in the output.

Table 3. Accuracy assessment of the inverse transient flow problem for 2007–2022 (in meters).

Well Number	3	14	107	1517	1537	1543	1550	Average
Max difference	0.8	0.9	0.5	0.8	0.8	0.8	0.6	0.74
Average difference	0.3	0.19	0.3	0.54	0.06	0.05	0.06	0.21
Coefficient of determination (R^2)	0.05	0.24	0.31	0.42	0.58	0.27	0.05	0.28
Average absolute deviation (MAD)	0.36	0.57	0.38	0.30	0.44	0.21	0.16	0.35
Mean absolute error (MAE)	−0.25	−0.19	0.30	0.50	0.09	0.07	−0.05	−0.16
Root mean square error (RMSE)	0.92	0.72	1.11	0.13	0.31	0.26	0.18	0.52

Table 4. The groundwater flux balance for 2013 and 2022 calculated for the Zhem Basin.

	Balance Items	2013		2022	
		Thousands m^3/Day	%	Thousands m^3/Day	%
Input	Storage recharge	4519	58.9	2408	34.5
	Recharge	3098	40.4	4514	64.7
	River leakage	49.9	0.7	53.2	0.8
	Total input	7667	100	6975	100
Output	Storage discharge	1438	18.4	1927	25.5
	Groundwater withdrawal	72.9	0.9	36.3	0.5
	Groundwater discharge to rivers	393	5.0	397	5.2
	Evapotranspiration	5942	75.7	5189	68.8
	Total output	7846	100	7549	100
	Input–output	−180	2.3	−573	8.2

The maximal groundwater withdrawal flux balances were calculated for 2013 and 2022, which is the end of the model identification period (Table 4). The balances were calculated for the entire model area and separately for freshwater development zones and salty and brackish water development zones in the southwestern part of the basin, according to the hydrogeological sketch (Figure 2).

The primary groundwater flow and storage reserve recharge is from precipitation, mainly in unconfined zones, which account for up to 99% of the input components. Increasing water withdrawal conditions and decreased annual precipitation in 2013 depleted the storage reserves, which reached a minimum in the 2012-2013 hydrological year. In the output balance items, evapotranspiration is predominant, accounting for up to ¾ of the output. Groundwater withdrawal account for only 1% of the total output, and groundwater discharge into rivers does not exceed 5–6%. The total groundwater flow rate of the Zhemsky Basin during these years was approximately 6500–7500 thousand m^3/day. The groundwater flow balance component ratio calculated for the freshwater distribution zone for the same periods of time (Table 5) is essentially the same as that calculated for the entire Artesian Basin area.

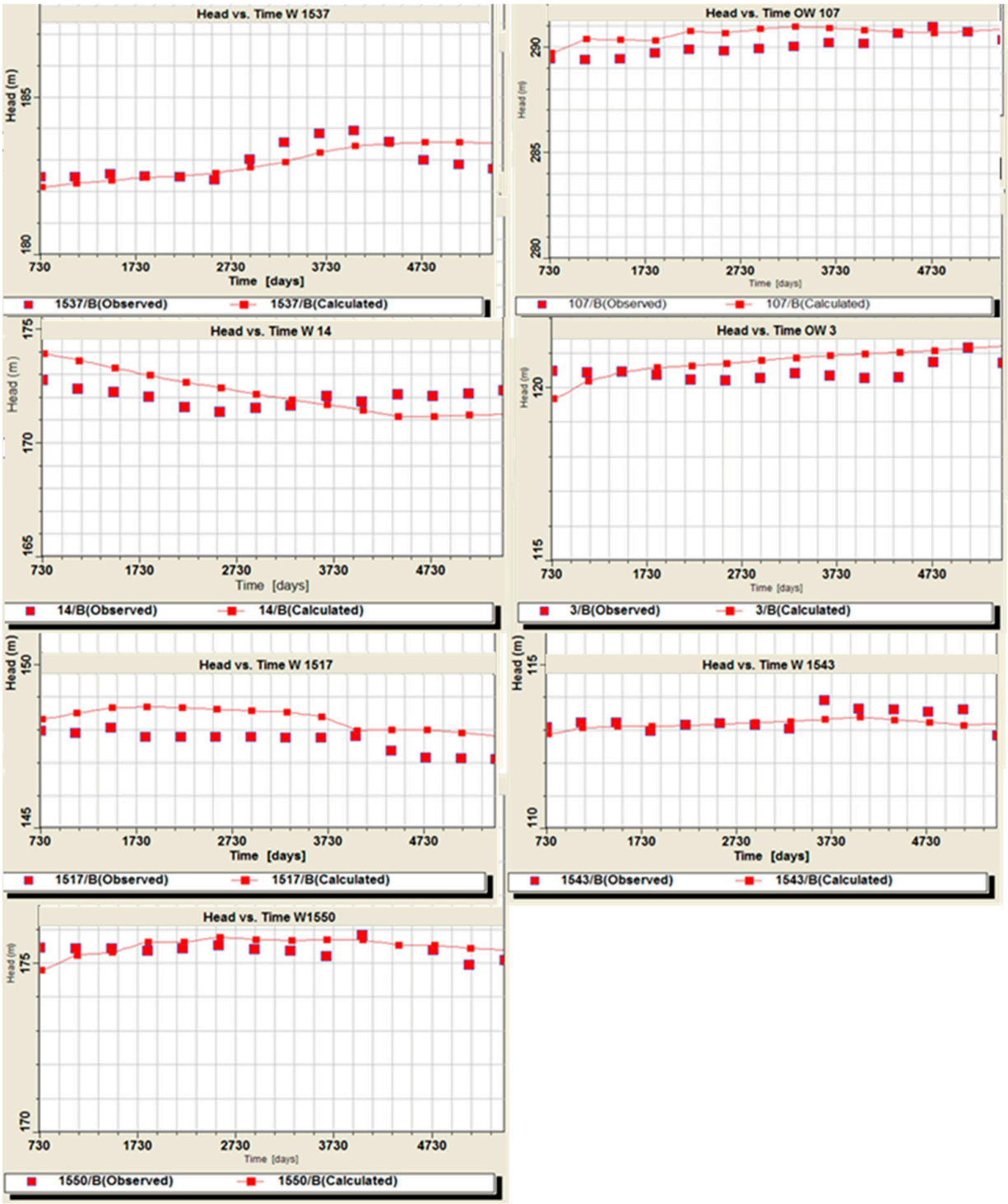


Figure 12. Model calibration vs. observed groundwater head fluctuations in the observation wells used for model calibration (Table 3). The general groundwater flow direction coincides with the relief slope in a westerly direction towards the Caspian Sea. The flow line direction near rivers characterizes groundwater recharge or discharge areas from/to the river. The pumping field and water well influence the groundwater flow, and the influence of the block structure (trough) is visible. The groundwater flow hydrodynamic gradient is 0.0013 on average and ranges from 0.0026 to 0.0006 depending on topographic conditions and the filtration capacity (Figure 14). Negative values in the groundwater depth model indicate areas with artesian confined groundwater flow conditions (Figure 15). These areas are located in low-relief areas and along river valleys, whereas elevated relief areas are phreatic.

Table 5. Fresh groundwater distribution zones and groundwater flux balance calculated for 2013 and 2022.

	Balance Items	2013		2022	
		Thousands m^3/Day	%	Thousands m^3/Day	%
Input	Storage recharge	1884	49	1229	25.5
	Recharge	2433	50	3562	73.5
	River leakage	37.6	0.8	41.1	0.8
	Influx from a brackish groundwater zone	9.2	0.2	10.1	0.2
	Total input	4363	100	4842	100
Output	Storage discharge	1115	26.0	1479	31.9
	Groundwater withdrawal	72.9	1.7	36.3	0.8
	Groundwater discharge to rivers	389	10	366.	7.9
	Evapotranspiration	2610	61.3	2717	58.8
	Outflow to a brackish groundwater zone	29.4	0.7	30.2	0.6
	Total output	4217	100	4629	100
	Input–output	146	3.3	213	4.4

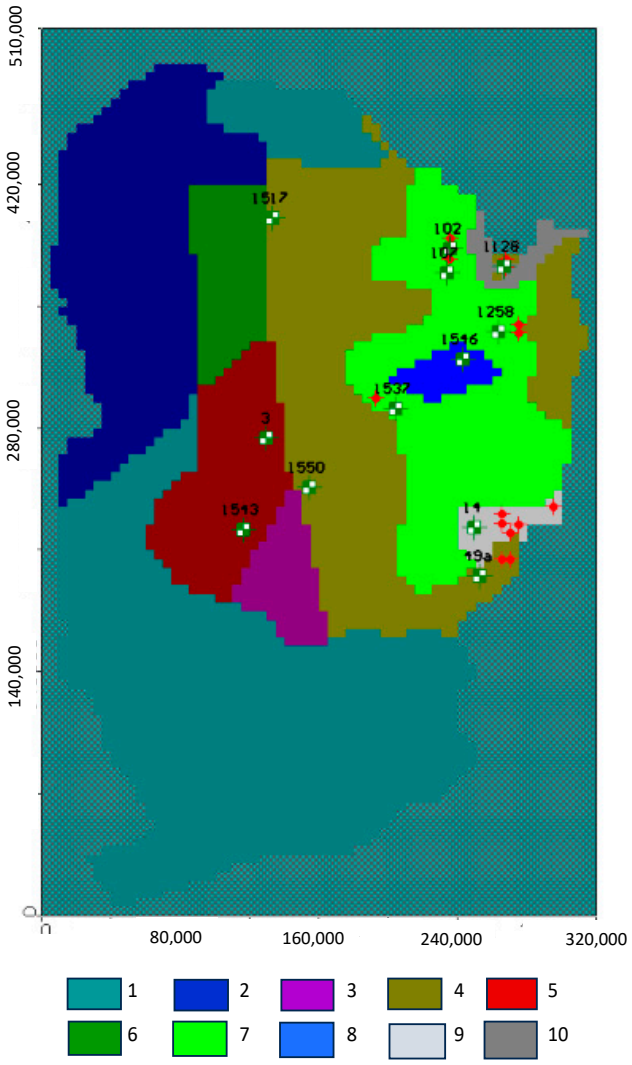


Figure 13. The calibrated hydraulic conductivity of the Zhem Basin model in m/day. 1—0.7; 2—1.0; 3—1.5; 4—2.0; 5—2.1; 6—3.0; 7—3.5; 8—4.0; 9—6.0; 10—8.0. Other symbols are shown in Figure 4.

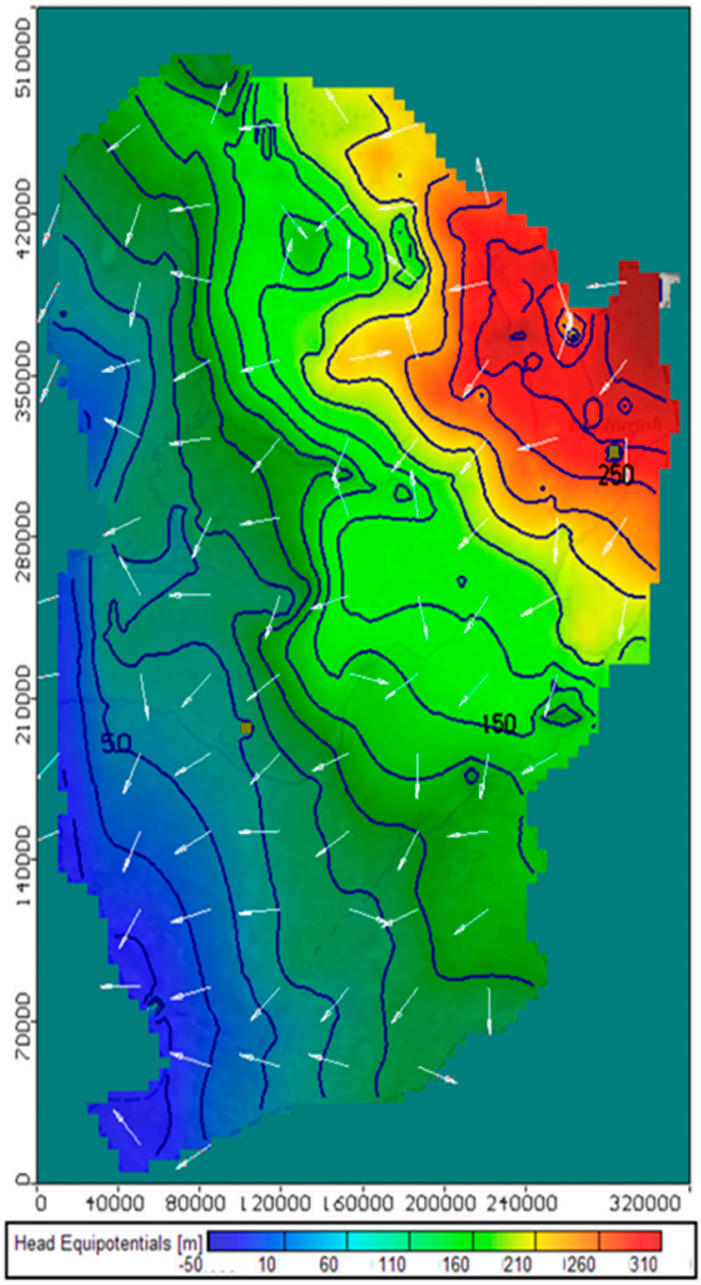


Figure 14. Groundwater head contours and flow path, 2022.

The total balance input characterizing the groundwater flow rate in the freshwater distribution zone is approximately 4500 thousand m^3/day, or 65% of the groundwater flow rate flux throughout the Zhem Basin. The groundwater outflows into the brackish water zone are relatively small, amounting to approximately 30 thousand m^3/day, which is approximately three times greater than the inflow from the brackish water zone into the freshwater zone. Almost all groundwater discharge to rivers is formed in the fresh groundwater distribution zone. The difference between the balance components calculated for the entire basin area and the freshwater distribution zone corresponds to the distribution zone balance components of predominantly brackish groundwater.

The model accurately simulated the measured historical characteristics of the simulated system, including hydraulic conductivity, specific storage, recharge, and groundwater balance values that concurred with the values obtained from field investigations within the specified modeling accuracy.

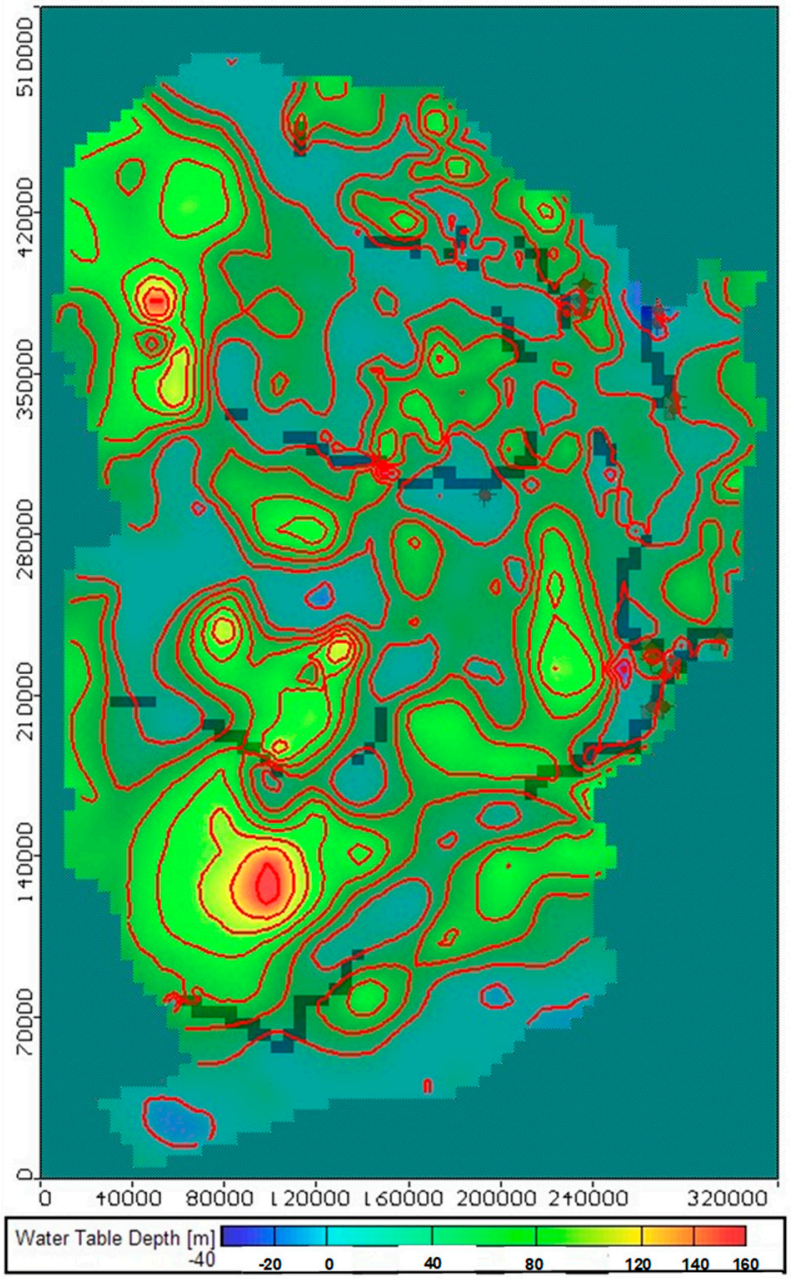


Figure 15. Groundwater depth, 2022.

3.2. Prediction Model

3.2.1. Initial Prediction

The hydrodynamic groundwater flow characteristics for 2070 will remain virtually unchanged (Figure 16), with the flow directions and hydraulic gradients preserved. Under long-term water withdrawal, recharge, and groundwater discharge conditions, the groundwater flow will stabilize to steady-state conditions. There may be slight changes in the drawdown within the existing water extraction influence radius. Figure 17 shows the groundwater head drawdown prediction around the Kokzhide (including the Emba wellfield) and Kenkiyak aquifer segments, suggesting that, by 2070, an ellipsoidal drawdown depression will occur, elongated in a northeast direction up to 35 km long and 20 km wide. Drawdowns in the depression center have reached 40–50 m, and those in the Alga water intake area reached 25–30 m from the groundwater head in 2007.

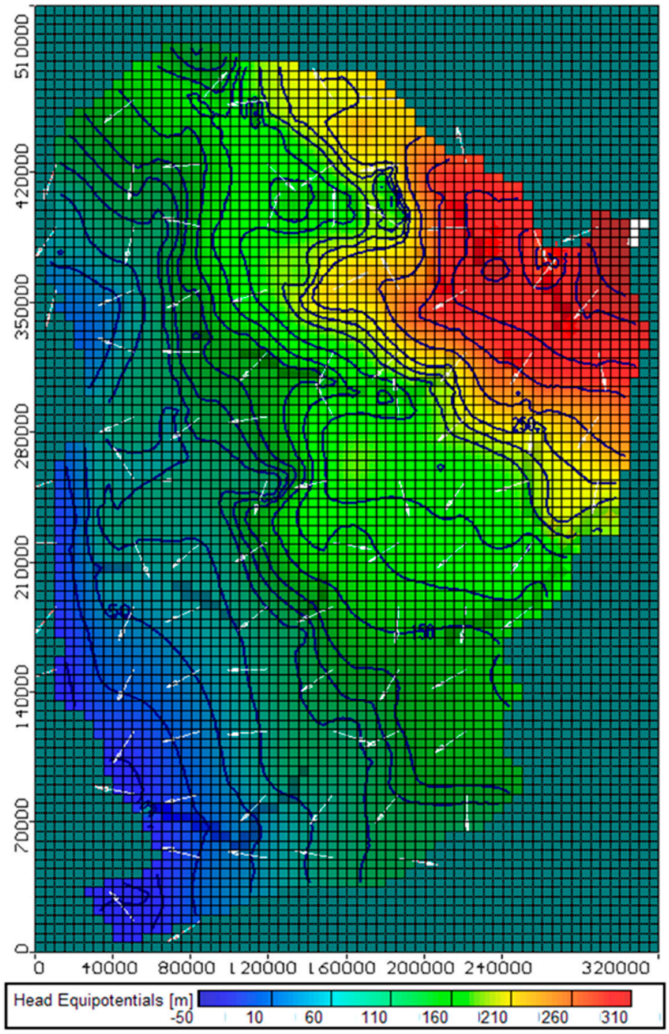


Figure 16. Initial prediction. Groundwater head contours and flow path, 2070.

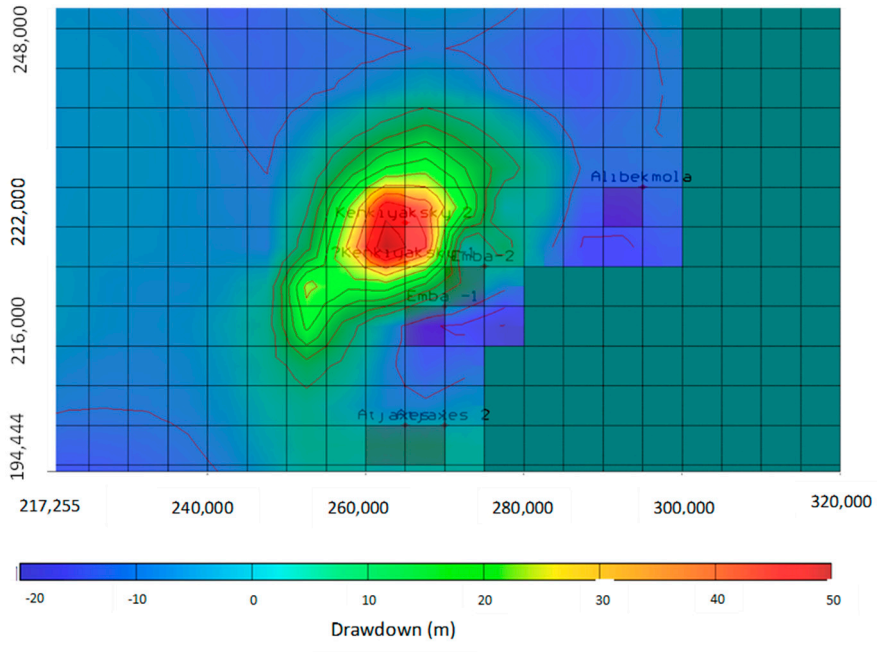


Figure 17. Initial groundwater heads drawdown prediction around the Kokzhide aquifer segment, including the Emba and Kenkiyak groundwater extraction areas, in 2070.

The groundwater flow balance model for 2070, compared with that for 2022, indicates that the balance will rely almost entirely on atmospheric precipitation (97% recharge). Groundwater resource replenishment by river recharge will not exceed 1%, and storage reserve balance will not exceed 2% of the total balance. Evapotranspiration and storage discharge will constitute more than 90% of the output components, whereas river discharge will remain at approximately 8%. In total, 5500–6000 thousand m^3/day of groundwater resources will be formed annually in the Artesian Basin territory, which is approximately 15% less than that in 2022.

3.2.2. Assessment of Exploitable Groundwater Resources in the Zhem Basin—Second Scenario Prediction

The predictive groundwater head contours and flow paths for 25 years are presented in Figure 18A, and those for 50 years are presented in Figure 18B. While the groundwater flow hydrodynamic pattern and main flow direction will remain similar, the hydraulic gradients will decrease in the northwestern part of the basin, where most of the groundwater reservoirs exist. Intensive extraction of groundwater will lead to a head decreasing below the earth's surface in areas where artesian conditions for the movement of groundwater develop, the cessation of self-flow from wells, and the formation of unconfined or low-pressure conditions of the groundwater flow. An extensive drawdown will form and increase over time in the Emben groundwater aquifer complex (Emba, Kenkiyak, Kokzhide, Atzhaksy, Alibekmola, and Kozhasay), which will reach 50–55 km in length and 30–35 km in width (Figure 19). The maximum predicted groundwater head drop will occur around two centers: the first is in the Kenkiyak deposit area, with decreases of 45–55 m by 2047 (25 years) and 60–65 m by 2070 (50 years), and the second is in the Kokzhide area, with a predicted drawdown of 40–45 m in 25 years and 50–55 m in 50 years. The ellipsoid shape of the depression is due to the linear arrangement of a large groundwater extraction area stretched along the Emba River valley, as well as the higher filtration properties of the aquifer in this area.

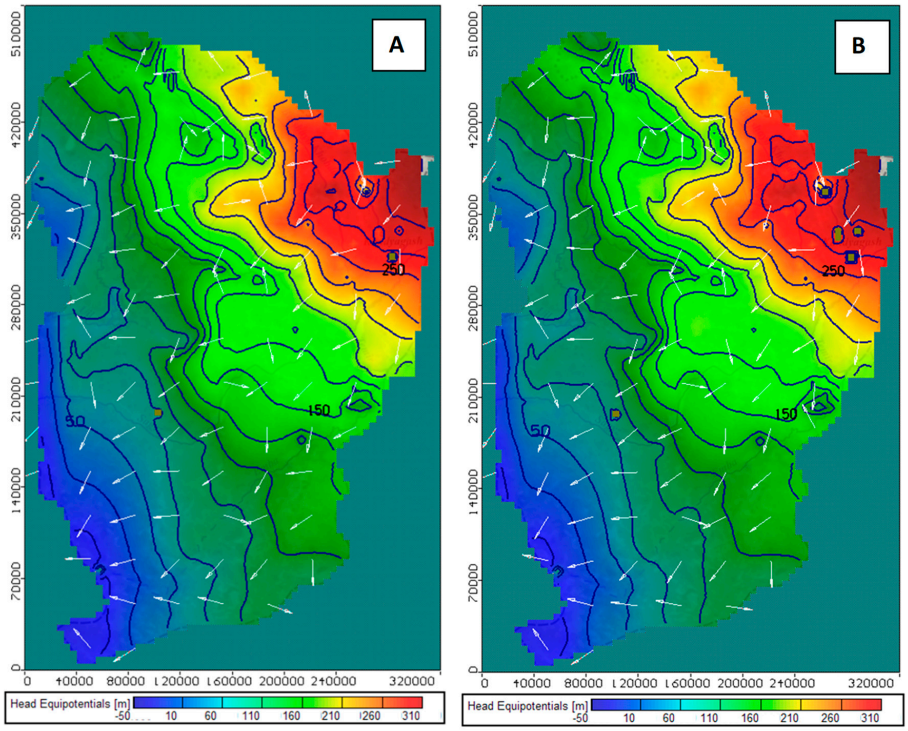


Figure 18. Second scenario prediction. Groundwater head contours and flow paths for 25 years (**A**) and 50 years (**B**).

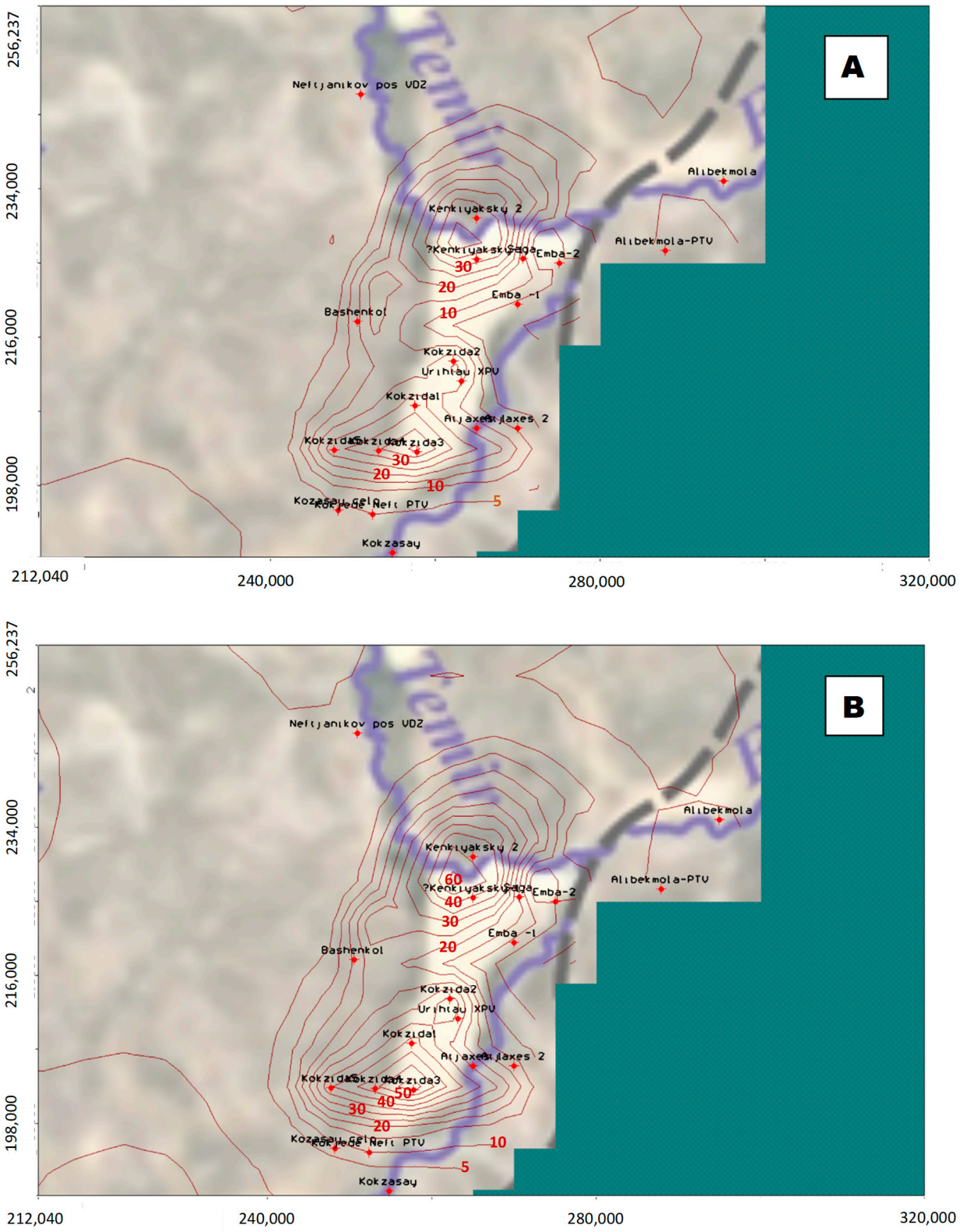


Figure 19. The second scenario drawdown prediction in the Emben aquifer complex for 25 years (**A**) and 50 years (**B**).

The Sarybulak aquifer complex is located in the northeast Zhem Basin, in the upper reaches of the Bolshaya, Malaya Khobda, and Temir rivers. The 25-year prediction (Figure 20A) suggests the formation of seven separate rather large drawdown funnels, namely Alginskoye–Bogdanovskoye, Kundaktykirskoe, Moiseevskoe, Sarybulakskoye–

Shubarsayskoye–West Kandygachskoye, Kandagachskoe, Dzhurun PTV, and Zharykskoe. A maximal drawdown exceeding 45 m is predicted in Bogdanovskoye, and a maximum drawdown of 15 to 35 m is predicted in the other locations. At the Dzhurun PTV wellfield, the predicted groundwater heads will drop below the modeled layer, i.e., the aquifer will drain completely. For the 50-year forecast period (Figure 20B), the Moiseevskoye and Sarybulak–Shubarsay–Kandygachsk West field drawdowns merged into an area of 40 km by 20 km. In the depression center, the drawdown will increase by 15–20 m compared with the 25-year forecast period. Notably, after 25 years, the wellfield of the Keregen-Sagyz aquifer and the Sagyz River has completely drained, and after 50 years, the wellfields of Bogdanovsk, Kandagach, and Zharyk have also increased.

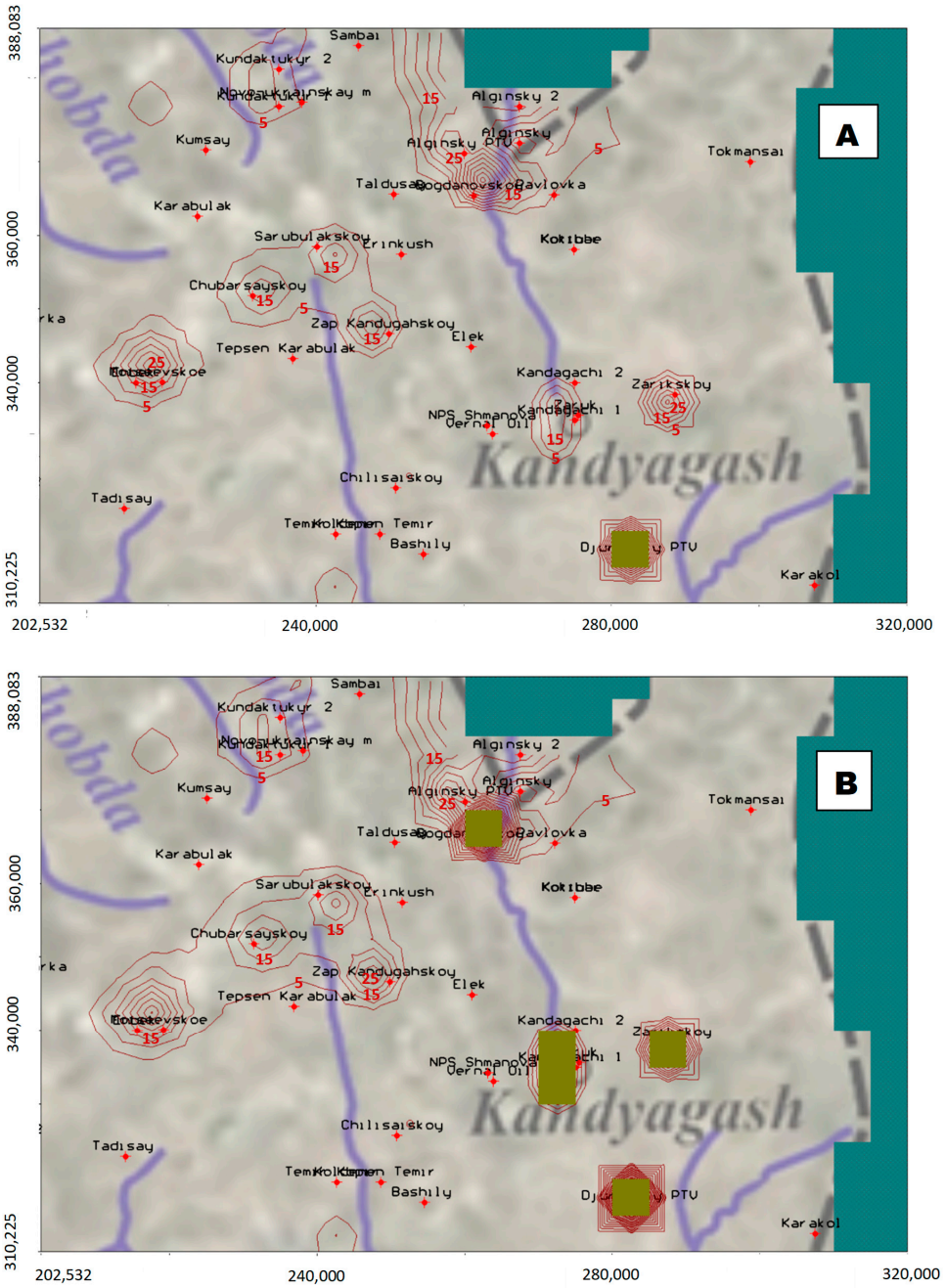


Figure 20. The second scenario predicts a drawdown in the Sarybulak aquifer complex area for 25 years (**A**) and 50 years (**B**).

The calculated maximal predicted groundwater head drawdowns have been developed since 2022 (Table 6), with both currently utilized and approved groundwater reserves exceeding 20,000 m^3/day. The calculations compensate for an additional decrease in the water head, enabling the computation of the cell area transition cuts to the actual average water drawdown radius. For most large groundwater aquifers (Table 6), the maximal model-calculated drawdowns did not reach the maximal permissible drawdowns. While model calculations confirm the approved exploitable groundwater volume, there are exceptions for the following segments: Kenkiyak, Kandagach, Zharkamys, and Dzhurun PTV. The exploitable groundwater resources (for water pumping) calculated for these areas were previously overestimated, since their interaction during simultaneous operation was not taken into account. The prediction calculations performed in this study suggest a reduction in the exploitable sustainable reserve. Calculations of possible water pumping, taking into account the maximum permissible drawdowns, are given in Section 3.2.3.

Table 6. Maximum predicted drawdowns in groundwater heads in comparison with permissible drawdown.

Deposit	Approved Exploitable Groundwater Resources, m^3/Day	Permissible Drawdown Accepted When Assessing Approved Exploitable Groundwater Resources, m	Maximum Model Predicted Drawdown, m		Additional Drawdown Correction, m	Maximum Predicted Drawdown with Correction, m		Difference Between Permissible and Maximum Predicted Drawdown, m	
			25 Years	50 Years		25 Years	50 Years	25 Years	50 Years
Emba	27,000	150	16.3	24.1	1.2	17.5	25.3	133	125
Kokzhide	173,400	67	39.8	57.8	2.1	41.9	59.9	25.1	7.1
Kenkiyak	21,600	59.9	70.4	82.2	3.3	73.7	85.5	−13.8	−25.6
Alibekmola	12,000	96	0.2	1	7.1	7.3	8.1	88.7	87.9
Alga	24,300	16.6	3.7	6.5	3.5	7.2	9.2	9.4	7.4
Kundaktur	46,656	100	22.3	25.6	0.3	22.6	15.8	77.4	84.2
Atzhaksy	40,450	88.8	29.1	43.7	4.3	33.4	44.4	55.4	44.4
Kandygach	23,760	36.8	38.9	59.7	2.5	41.4	62.2	−4.6	−25.4
Shubarkudyk	2820	19	2.6	3.4	3.1	5.7	4.1	13.3	14.9
Moiseevskoye	45,000	103	32.6	38.2	38.7	71.3	76.9	31.2	25.6
Sarybulak	25,000	60	21.1	25.7	0.4	21.5	26.1	38.5	33.9
Alga PTV	24,300	39.3	20.8	35.5	2.7	23.5	38.2	15.8	1.1
Dzhurun PTV	40,200	57.2	86.1	167	83.3	169	250	−112	−193
Jarkamus	37,000	70	100	121	27.1	128	105	−57.5	−34.5
Kandygach West	29,300	48.5	25.7	33	0.3	26.0	33.3	22.5	15.2

The predictive groundwater flow balance changes according to the second scenario are presented in Tables 7 and 8. After 25 years of groundwater utilization operations, exploitable groundwater resources will withstand the approved limits, with a total flow rate of 6087 thousand m^3/day, which is almost 90% of the precipitation input. Leakage losses from rivers will double to approximately 104,000 m^3/day, which will not deplete or gain storage reserves. Nonetheless, lowering the groundwater head might lead to drawdowns. The groundwater head drop will reduce evapotranspiration [43] from approximately 70% (2022) to 1100 thousand m^3/day (18%). In the 50-year prediction, the drawdown development stabilizes, as groundwater discharge slightly decreases (by approximately 4%). With balance components generally alike across the entire basin, river leakage will increase approximately twofold during the 25-year predictive period, with a subsequent reduction during the stabilization period (50-year prediction). Groundwater discharge into rivers will be reduced by almost 50 thousand m^3/day and the groundwater flow rate will be approximately 4600 thousand m^3/day, or approximately 75% of the Zhem Artesian Basin.

Table 7. The groundwater flux balance of the Zhem Basin, calculated over prediction periods of 25 and 50 years. Second scenario prediction.

	Balance Items	25 Years		50 Years	
		Thousands m^3/Day	%	Thousands m^3/Day	%
Input	Storage recharge	636	10.5	406	6.9
	Recharge	5347	87.8	5347	91.3
	River leakage	104	1.7	105	1.8
	Total input	6087	100	5858	100
Output	Storage discharge	3871	64.4	3559	61.7
	Groundwater withdrawal	715	11.9	715	12.4
	Groundwater discharge to rivers	352	5.8	351	6.2
	Evapotranspiration	1081	17.9	1138	19.7
	Total output	6020	100	5764	100
	Input–output	67.2	1.1	94.9	1.6

Table 8. Fresh groundwater distribution zone flux balance is calculated for prediction periods of 25 and 50 years. Second scenario prediction.

	Balance Items	25 Years		50 Years	
		Thousands m^3/Day	%	Thousands m^3/Day	%
Input	Storage recharge	552	11.6	383	8.4
	Recharge	4118	86.3	4118	90.3
	River leakage	91.8	1.9	49.3	1.1
	Influx from a brackish groundwater zone	7.7	0.2	7.8	0.2
	Total input	4769	100	4558	100
Output	Storage discharge	2777	59	2505	55.5
	Groundwater withdrawal	702	14.9	702	15.5
	Groundwater discharge to rivers	320	6.8	315	6.9
	Evapotranspiration	875	18.6	965	21.3
	Outflow to a brackish groundwater zone	32.8	0.7	34.4	0.8
	Total output	4706	100	4521	100
	Input–output	62.8	1.3	36.4	0.8

3.2.3. The Third Prediction Scenario Aims to Determine the Maximum Possible Water Withdrawal at Which the Predicted Groundwater Head Drawdown Will Not Exceed the Permissible Values

The calculations included the following groundwater reservoirs: Kenkiyak, Kandagach, Dzhurun PTV and Zharkamys. The exploitable groundwater resources and the resulting maximal groundwater head drawdown modeling consider the adjusted corrections (Table 9). While the approved exploitable groundwater resources for these four aquifer segments are 122,560 m^3/day, the model calculates that exploitable groundwater resources, with maximal permissible drawdown, amount to just 37,000 m^3/day. The aquifer's dynamic model indicates that the decrease in the total water withdrawal on the Bogdanovsk, Zharyk, and Keregen-Sagyz segments will not completely drain them. Thus, the total exploitable groundwater resources of the Upper Cretaceous and Quaternary sediments of the Zhem Artesian Basin will be 629,400 m^3/day.

Table 9. The model calculates exploitable groundwater resources.

Deposit	Exploitable Groundwater Resources, m^3/Day	Maximal Permissible Drawdown, m	Additional Drawdown Correction, m	Maximum Calculated Drawdown with Correction, m	
				25 Years	50 Years
Kenkiyak	4000	59.9	1.4	52.7	60.2
Kandagach	16,000	36.8	2	30.7	38.9
Dzhurun PTV	11,000	57.2	30	50.6	54.7
Zharkamys	6000	70	5	67.3	69.3

The limitations of the created model are related to the grid spacing, time discretization, parameter structure, insufficient calibration data, and the effects of processes not simulated by the model. These factors, along with unavoidable errors in observations, result in some uncertainty in model predictions. Thus, the size of the computational block of the model (5 × 5 km) does not allow modeling pumping from a single well, but only from a water wellfield of significant dimensions. Combining several aquifers into one model layer does not provide the ability to reproduce water extraction from different depths of filter installation, as well as the variability in filtration properties vertically in the sediment section. The time step size of 1 year does not allow for seasonal fluctuations in groundwater heads. However, given the stated aims of the model, these limitations do not have a significant impact on the reliability of the prediction solutions.

3.2.4. Prospects for Utilizing Cretaceous Groundwater Resources as a Water Supply

Water withdrawal for household and drinking purposes in the most water-scarce administrative regions of western Kazakhstan in 2021 was (in m^3/day) 112,190 in Aktobe, 122,070 in Atyrau, and 969,900 in Mangistau. From a total water withdrawal of 331,000 m^3/day, 140,000 m^3/day was accounted for by groundwater, while the remaining demand was covered by surface water (in the Mangistau and Atyrau regions). Moreover, the total demand for these administrative units in 2010 was 640,360 m^3/day, almost twice the actual water withdrawal in 2021. At the same time, the estimated river flow reduction by the model at the end of the forecast period (50 years) is about 77 thousand m^3/day, which is less than 4% of the total river flow. The prospective water demand in these administrative regions for 2030, 2050, and 2070 is shown in Table 10. The prospective demand for drinking water in three administrative regions of western Kazakhstan, oriented towards the groundwater basin for 2030, 2050, and 2070, was estimated based on the trend of increasing total water consumption due to population growth and improvements to the water infrastructure, as well as taking into account prospective plans for the development of economic sectors [44].

Table 10. Prospective water demand for domestic and drinking water supply, thousand m^3/day.

Administrative Region	2030	2050	2070
Aktobe	321	355	393
Atyrau	195	223	253
Mangistau	201	226	255
Total	**717**	**804**	**901**

By 2070, the freshwater demand for domestic and drinking water supply will increase from 640,000 to 901,000 m^3/day, where the maximum groundwater usage for household and drinking water supply is in the Aktobe region. The exploitable fresh groundwater resources in the Mangistau and Atyrau regions are significantly smaller; therefore, their water supply is fulfilled to a greater extent from surface water, with treatment used to

improve their quality to the appropriate standards. Full surface runoff utilization is restricted in these regions since a significant portion is accounted for mandatory release to neighboring countries, evaporation and filtration losses, environmental sanitary releases to the lower reaches of rivers, and other runoff losses. The runoff available for use in low-water level years (95%) for the entire Aktobe region is only 0.12 km^3/year, which is less than the prospective need for 2070 (Aktobe and Atyrau regions), which will amount of 612.6 thousand m^3/day or 0.22 km^3/year.

Consequently, such water withdrawal will lead to a decrease in river flow and wetland extent and to environmental degradation. As such, the most promising water supply for both areas is the fresh and slightly brackish groundwater of the Zhem Artesian Basin Albian–Cenomanian aquifer complex. At the same time, the exploitable groundwater resources with mineralization of 1–3 g/L are 12,400 m^3/day or 2% of their total amount. In conditions of an acute deficit of water resources in the western regions of the Zhem Artesian Basin, these waters can be used for the domestic and drinking water supply of small villages and the watering points of distant pastures in accordance with the directive documents of the Kazakhstan Republic. The corresponding project for transferring part of the exploited groundwater resources from the Zhem Artesian Basin, Albian–Cenomanian aquifer complex, to water-deficient areas of the Mangistau and Atyrau regions is in the development stage.

Based on the Zhemsky artesian basin exploration and assessment results, groundwater reserves are confined to the Albian–Cenomanian aquifer complex, and using modern filters and gravel backfill of the annular space, sand removal by production wells and, accordingly, land subsidence [9] were not noted [20–24]. Thus, there is every reason to assume that these negative phenomena will not occur during the construction and operation of new water wellfields, which is confirmed by the operating experience of large wellfields, such as Emba, Kenkiyak, Atzhaksy, Alibekmola and Kandagach. The Zhem Artesian Basin deep high-quality aquifer complex is overlaid by low-permeability clay layers and is not subject to a contamination risk. The long-term wellfield operation experience and groundwater quality monitoring data reveal stability in their chemical composition and the absence of contamination.

At the same time, in areas where groundwater has unconfined conditions and wellfields are located near industrial facilities, there is a potential risk of contamination. In this case, it is advised that a sanitary protection zone around the wellfield should be created [45]. When new wells are put into operation and groundwater withdrawal is intensified, the contamination risk increases. This requires constant monitoring of the pumped water quality. Taking into account the depth of the Albian–Cenomanian aquifer complex, a decrease in groundwater pressure head during the pumping well operation does not have any significant impact on vegetation and river runoff [20–24]. At the same time, according to the Code of the Republic of Kazakhstan "On Subsoil and Subsoil Use" (https://adilet.zan.kz/rus/docs/K1700000125, accessed on 20 April 2025), state monitoring of groundwater is carried out at exploited aquifer segments, including observations of river runoff. Consequently, when new wells are put into operation in the future, monitoring will be carried out, and the impact of increased water withdrawal on the environment will be assessed.

The cost of 1 m^3 of pumped groundwater, according to the Department of State Revenues in Kazakhstan, is USD 0.4. The cost of groundwater exploration carried out from 2002 to 2021, calculated for 25 years of water withdrawal operations of the Zhem Artesian Basin10 largest well fields, was on average USD 0.28 per 1 m^3. At the same time, the cost of 1 m^3 of water for the urban population of Aktobe, whose water supply is groundwater-based, is USD 0.42. For comparison, the cost of 1 m^3 of water for the cities

of western Kazakhstan, whose water supply is surface water-based, is USD 0.97. Thus, groundwater supply to the regions of western Kazakhstan is economically viable and often the only way of providing this resource.

4. Conclusions

Owing to global climate change aligned with a general increase in human environment standards, freshwater demand is increasing both globally and, in particular, in western Kazakhstan. As the region's demand for water will increase from 640,000 to 901,000 m^3/day by 2070, the Zhem Artesian Basin groundwater is planned to fill the demand to supply the identified deficiency. The Aktobe region has significant groundwater resources of up to 755,000 m^3/day due to the Cretaceous Albian–Cenomanian aquifer complex. To date, exploitable groundwater resources have been approved for 123 aquifer segments and individual wellfields, with 173,000 m^3/day overall.

While previous work used segmented numerical groundwater flow modeling to assess the Zhem Artesian Basin cretaceous aquifer exploitable groundwater resource, the present work modeled it as an aquifer complex. The modeling process consisted of assessing and reassessing groundwater resource datasets and monitoring data that supported the computer model's training, calibration and validation, in order to attain several simulated predictions. The prediction results for 25 and 50 years suggest that the long-term exploitable groundwater resources of the basin are 629,400 m^3/day.

The main specific conclusions from the scenario prediction results suggest the following:

- The hydrodynamic characteristics of groundwater flow in 2070 will remain similar to the conditions prevailing in 2022;
- In most aquifer segments, the maximum model-calculated drawdowns were less than the maximum permissible drawdowns and, therefore, the segments are exploitable groundwater resources;
- The entire Zhem Basin's annual renewable groundwater resources amount to approximately 6087 thousand m^3/day, 75% of which are in the freshwater development zone;
- The simultaneous extraction of all approved exploitable groundwater resources is predicted to result in the development of extensive drawdown funnels with depths of up to 50–80 m, which will reduce surface river flow to approximately 110 thousand m^3/day (about 6% of the average long-term river flow).

Considering the above, the following applicative recommendations and limitations are acknowledged:

- Groundwater resource utilization is advisable for a stable, high-quality drinking water supply to the Atyrau and Mangistau residents, including through its transfer from the adjacent Aktobe region;
- The 630,000 m^3/day drinking-quality groundwater potential may serve more than 70% of the future water demand of the three regions;
- Developing a more detailed water resource management scheme should consider economic criteria. For that matter, additional work is recommended, including mapping the customer pipeline construction cost;
- Mineralization of up to 3 g/L might restrict the reservoir's utilization; nonetheless, according to the current water supply regulations in Kazakhstan, it is one of the primary potential water sources.
- Since the Kenkiyak, Kandagach, Zharkamys, and Dzhurun PTV groundwater head drawdowns might exceed the permissible values, their exploitable groundwater resources potential is reduced from 122,560 m^3/day to 37,000 m^3/day.

The created model of the artesian basin is supposed to be used in the future for the operational assessment of groundwater reserves of newly explored areas. In combination with programs for optimal water resource management (for example, WEAP), it will serve as a reliable tool in designing the groundwater resources transfer to adjacent water-deficient areas of western Kazakhstan.

The developed methodological approaches will be used to assess the exploitable groundwater resources of large artesian basins using modeling methods in Kazakhstan and other countries.

Author Contributions: Conceptualization and methodology, V.M. and D.S.S.; model compilation, V.M. and D.S.S.; formal analysis and results' validation, V.M., Y.Z.M., and V.A.S.; resources and data curation, D.S.S.; writing—original draft preparation, V.M. and D.S.S.; writing—review and editing, Y.A. All authors have read and agreed to the published version of the manuscript.

Funding: This research was funded by the Science Committee of the Ministry of Science and Higher Education of the Republic of Kazakhstan (Grant No. BR 21882211). The authors are grateful to all the organizations and individuals who provided the data and provided motivation to finish the article.

Data Availability Statement: The research data are available upon request.

Conflicts of Interest: The authors declare no conflicts of interest.

Appendix A. General Characteristics of the Groundwater Chemical Content of the Albian–Cenomanian Aquifer Complex Based on the Results of the Abbreviated Chemical Analysis

Water Chemical Component, mg/L	TDS < 1 g/L 37 Water Samples (69% from Total)			TDS from 1 to 3 g/L 7 Water Samples (13% from Total)			TDS from 3 to 10 g/L 10 Water Samples (18% from Total)		
	Min	Max	Average	Min	Max	Average	Min	Max	Average
TDS	0.2	1	0.5	1.4	2.8	2.2	3.5	9.7	5.65
pH	6.5	8.5	7.2	7.4	7.8	7.5	7	8	7.4
Total hardness, mg-eq/L	1.31	9	3.7	10.03	35	21.1	11.2	94	33.5
$(Na + K)^+$	3	231	90	165	620	382.3	786	2777	1326.9
Ca^{2+}	17	101	47.8	108	216	171.3	24	1343.3	346.3
Mg^{2+}	0	91	19.5	45	146	104.5	2.06	547.2	207.4
Fe	0	0.97	0.05	-	-	-	-	-	-
Cl^-	4	213	75.5	366	896	770.3	1165	4751.6	2408.3
SO_4^{2-}	18.9	379	122.5	213	880	531.8	651.66	1915	1173.7
HCO_3^-	11	400	190.6	192	268	227.7	119	293	219.8

Appendix B. Characteristics of the Groundwater Chemical Content of the Albian–Cenomanian Aquifer Complex for Compliance with SP-26 (Requirements for Drinking Water)

Parameter	Unit	Maximum Permissible Concentration According to SP-26	Min	Max	Average
Smell (20 °C)	Score (point)	2	0	2	0.2
Aftertaste (20 °C)	Score (point)	2	0	2	0.2
Color	Degree	20 (35)	0.6	20	5.3
Мутность	mg/L	1.5 (2)			
pH	-	6–9	7.05	8.8	7.7

Parameter	Unit	Maximum Permissible Concentration According to SP-26	Min	Max	Average
Oxidizability	mg/L	2 (5)	0.4	2.5	1.0
NH_3	mg/L	2.0	0	0.63	0.05
NO_2	mg/L	3.0	0	0.09	0.009
NO_3	mg/L	45	0	10.4	1.6
Total hardness	mg-eq/L	7.0 (10)	0.8	8.25	3.7
TDS	mg/L	1000 (1500)	105	863	456.8
Cl^-	mg/L	350	4.6	270	71.8
SO_4^{2-}	mg/L	500	10	241	102.5
Fe	mg/L	0.3 (1.0)	0	0.9	0.15
Cu	mg/L	1.0	0	0.5	0.03
Cd	mg/L	0.001	0	0.0004	0.0001
Zn	mg/L	5.0	0	0.12	0.04
Pb	mg/L	0.03	0	0.021	0.0045
Mo	mg/L	0.25	0	0	0
Be	mg/L	0.0002	0	0	0
Mn	mg/L	0.1 (0.5)	0	0.09	0.02
B	mg/L	0.5	0	0.303	0.1
Se	mg/L	0.05	0	0.46	0.09
Cr	mg/L	0.05	0	0	0
F	mg/L	1.5	0.02	1.45	0.5
Ni	mg/L	0.1	0	0.04	0.008
Co	mg/L	0.1	0	0.15	0.025
Sb	mg/L	0.05	0	0	0
As	mg/L	0.05	0	0.01	0.0003
Polyphosphates	mg/L	3.5	0	0	0
Ba	mg/L	0.1	0	0	0
Petroleum products	mg/L	0.1	0	0.08	0.04
Al	mg/L	0.5	0	0	0
Hg	mg/L	-	0	0	0
DDT	mg/L	0.002	0	0.002	0
HCH-γ (lindane)	mg/L	0.002	0	0.002	0
2,4 D-salt	mg/L	0.03	0	0.001	0
Total alpha (α) radioactivity	K − 1	0.2	0	0.186	0.033
Total beta (β) radioactivity	K − 1	1.0	0.01	0.647	0.099
Total viable count (TVC)	cfu/cm^3	Less than 50	0	20	5.6
Total coliform (TCB)	100 per 100 ml	Absence	0	0	0
Thermotolerant coliform bacteria (TCB)	100 per 100 mL	Absence	0	0	0

Appendix C. Geofiltration Parameters Obtained from Pumping Tests Performed During a Hydrogeological Survey in the Zhem Basin

Wellfield Name	Coordinate X in Model	Coordinate Y in Model	Hydraulic conductivity, m/Day (pumping Test)	Adequate Pumped Layer Thickness, m	Specific Storage (S_s)	Specific Yield (S_y)	Layer Thickness, m	Hydraulic Conductivity Averaged for the Layer Thickness, m/Day
Bashily	254,500	316,800	8	23	0.13		100	1.8
Aksay	136,500	425,300	3.6	16		0.001	136	0.4
Jambul	253,700	277,500	6	32		0.15	108	1.8
Sarubulasky	240,100	358,500	7.4	50.75	0.13	0.008	131	2.9
Laktubay	231,200	153,200	1.96	59		0.00069	212	0.5
Kokzhide	256,400	206,200	8.1	117.8	0.14		191	5.0
Ashikol	269,800	154,500	5.19	128.97		0.00068	350	1.9
Atzhaksy	264,300	202,600	9.5	96	0.14		128	7.1
Kojasay	254,800	189,900	8.9	76	0.14		171	4.0
Emba	264,300	215,500	7.3	200	0.14	0.00832	160	9.1
Alibekmola	287,900	226,500	9.6	63		0.00065	200	3.0
Kenkiyak	254,600	220,500	8.5	91	0.14	0.00001	143	5.4
Kakakuduk	209,500	412,400	4.2	32	0.14		98	1.4
Shandy	176,200	430,700	1	36.6	0.117		116	0.3
Sambay	245,700	385,700	11	18	0.1		85	2.3
Bulgarka	201,400	347,300	10.1	32.2	0.13		61	5.3
Saruhobda	194,300	364,800	8.1	28	0.11		108	2.1
Pavlovka	272,200	365,500	8.2	23	0.13		33	5.7
Altukarasy	151,700	303,900	5.6	21	0.14		135	0.9
Moiseevskoye	219,100	340,100	7.1	109	0.13	0.0037	226	3.4
Kundaktyr	235,100	378,000	5.1	101	0.13	0.0018	121	4.3
Karatube PTV	203,500	157,000	9.3	46		0.0015	205	2.1
Karatube XPV	203,500	157,000	10	11.7	0.14		205	0.6
Urintay	263,100	210,700	9.6	107	0.14		203	5.1
Sarybulak	143,600	372,600	7.48	60.94	0.1		80	5.7
Novo-Mihailovka	166,600	446,500	3	4		0.0048	77	0.2
Sazdy	237,200	405,300	7.1	17.1	0.1		32	3.8
Sambay	246,700	386,700	11	18	0.1		58	3.4
Saruhobda	194,000	364,600	8.1	28	0.11		102	2.2
Tamdy	258,800	368,700	7.83	43.77	0.15		60	5.7
Karabulak	223,900	362,600	7.1	58.5	0.13		114	3.6
Kazahstan	148,800	222,100	4.9	31		0.0008	297	0.5
Jarly	134,400	227,100	7.06	45		0.0063	108	2.9
Taldusay	153,700	412,600	5.1	40		0.005	119	1.7
Bestau	166,000	426,300	0.8	19.3		0.002	94	0.2
Dzhurun PTV	281,200	306,400	3.8	44.3	0.15		78	2.2
Aksay PTV	199,100	325,200	3.3	20.8	0.13		75	0.9
Tokmansay	298,800	370,000	1	25	0.12		67	0.4
Jarkamus	196,800	158,100	4.15	56		0.1	209	1.1
Kemershy	224,800	174,100	10.7	59		0.2	212	3.0
Ebeity	107,700	178,800	3.36	29	0.14		115	0.8
Karauilkeldy	150,100	245,100	7.34	40	0.1		242	1.2
Terisakan	148,700	432,900	3.1	66		0.01	142	1.4
Beltabanov	131,300	393,600	1.77	10.5		0.01	148	0.1
Karakol	307,500	312,600	1.1	27	0.12		108	0.3
Sagashily	238,400	314,900	27.2	6.6	0.19		63	2.8
Kunmkuduk	131,100	305,800	5.4	28	0.149		110	1.4
Shubarkuduk	198,700	288,700	9.3	51	0.14		101	4.7
Novo-Alekseevkoy	136,100	403,700	4	49.5		0.0005	142	1.4
Dijar	168,400	24,400	2.31	187.3		0.009	730	0.6
Karajal	180,600	148,800	2.6	38		0.0081	176	0.6
Kalinovka	117,500	386,700	5.32	48		0.0001	189	1.4
Jarsay	138,500	429,400	5.7	62		0.0075	136	2.6
Akjar	110,400	334,200	4.6	60.22	0.15		111	2.5
Karakuduk	209,500	412,400	4.2	32	0.14		98	1.4
Shady	174,900	430,200	1	36.6	0.117		100	0.4
Altay Batur	148,500	194,600	2.49	51.4		0.0015	63	2.0
Korashy	144,900	218,100	1.1	17.2		0.0002	214	0.1

Wellfield Name	Coordinate X in Model	Coordinate Y in Model	Hydraulic conductivity, m/Day (pumping Test)	Adequate Pumped Layer Thickness, m	Specific Storage (S_s)	Specific Yield (S_y)	Layer Thickness, m	Hydraulic Conductivity Averaged for the Layer Thickness, m/Day
Kokbulak	179,100	239,400	2.3	37.8		0.00022	180	0.5
Zharyk	275,500	335,600	3.9	20.2	0.14		44	1.8
Enbek	215,600	340,000	7.1	72		0.0037	226	2.3
Kumjargan	83,100	292,800	2	29.3	0.13		123	0.5
Kosembay	94,900	333,100	2.8	20		0.00022	132	0.4
Akshatau	47,700	308,900	2.4	33.7	0.13		195	0.4
Taskopa	134,600	261,100	4.3	75		0.04	120	2.7
Aksay	137,300	425,400	3.6	16		0.001	136	0.4
Jamsul	253,400	276,500	6	32	0.15		108	1.8
Akmolsay	180,800	451,600	14.1	9		0.01	219	0.6
Elek	261,000	344,900	10.8	25	0.16		58	4.7
Taldusay	214,000	323,000	4	20		0.01	96	0.8
Shugirly	179,500	349,000	3.4	16	0.14		79	0.7
Akkemer	81,300	346,400	2.2	10.5	0.13		153	0.2
Kursay	117,200	418,500	6.4	14		0.01	113	0.8
Jeruiyik	226,600	405,400	1.39	7		0.003	86	0.1
Taldusay	250,500	365,600	2	25	0.01		53	0.9
Kaindusay	208,100	415,000	10.5	12.5		0.044	98	1.3
Kosaral	162,100	229,300	5.16	10		0.0013	258	0.2
Kopa	99,400	184,600	4.2	20.9	0.15		134	0.7
Kozasay	243,900	186,100	1.9	82	0.13		170	0.9
Erkinush	251,500	357,400	12.7	17.35	0.06		88	2.5
Kumsay	225,000	371,600	5.1	38		0.06	93	2.1
Koktogay	197,400	402,200	3.2	22		0.047	104	0.7
Ashisay	186,500	353,700	4.1	18		0.001	118	0.6
Alga PTV	260,000	371,100	29.8	51.7	0.22		68	22.7
Temir	243,800	293,700	10.3	84.8		0.00238	182	4.8
Kandagach	263,800	334,400	6.9	42	0.13		63	4.6

References

1. Alelaimat, A.; Yusoff, I.; Nizar, M.K.; Ng, T.F.; Majali, Y.A. Groundwater Management in the Face of Climate Change: Enhancing Groundwater Storage in the Alluvium Aquifer of Wadi Araba, Jordan, through GIS-Based Managed Aquifer Recharge and Groundwater MODFLOW. *Water Supply* **2023**, *23*, 5136–5153. [CrossRef]
2. Ricart, S.; Villar-Navascués, R.A.; Hernández-Hernández, M.; Rico-Amorós, A.M.; Olcina-Cantos, J.; Moltó-Mantero, E. Extending Natural Limits to Address Water Scarcity? The Role of Non-Conventional Water Fluxes in Climate Change Adaptation Capacity: A Review. *Sustainability* **2021**, *13*, 2473. [CrossRef]
3. Mehta, L. Water and Human Development. *World Dev.* **2014**, *59*, 59–69. [CrossRef]
4. Izbicki, J.A.; Teague, N.F.; Hatzinger, P.B.; Böhlke, J.K.; Sturchio, N.C. Groundwater Movement, Recharge, and Perchlorate Occurrence in a Faulted Alluvial Aquifer in California (USA). *Hydrogeol. J.* **2015**, *23*, 467–491. [CrossRef]
5. Lu, Y.; Dai, L.; Yan, G.; Huo, Z.; Chen, W.; Lan, J.; Zhang, C.; Xu, Q.; Deng, S.; Chen, J. Effects of Various Land Utilization Types on Groundwater at Different Temporal Scales: A Case Study of Huocheng Plain, Xinjiang, China. *Front. Environ. Sci.* **2023**, *11*, 1225916. [CrossRef]
6. Sagin, J.; Adenova, D.; Tolepbayeva, A.; Poryadin, V. Underground Water Resources in Kazakhstan. *Int. J. Environ. Stud.* **2017**, *74*, 386–398. [CrossRef]
7. Akurugu, B.A.; Obuobie, E.; Yidana, S.M.; Stisen, S.; Seidenfaden, I.K.; Chegbeleh, L.P. Groundwater Resources Assessment in the Densu Basin: A Review. *J. Hydrol. Reg. Stud.* **2022**, *40*, 101017. [CrossRef]
8. Naik, P.K.; Awasthi, A.K. Groundwater Resources Assessment of the Koyna River Basin, India. *Hydrogeol. J.* **2003**, *11*, 582–594. [CrossRef]
9. Shen, Y.; Hesham El Naggar, M.; Zhang, D.; Huang, Z.; Du, X. Optimal Intensity Measure for Seismic Performance Assessment of Shield Tunnels in Liquefiable and Non-Liquefiable Soils. *Undergr. Space* **2024**, *21*, 149–163. [CrossRef]
10. Rojas, R.; Commander, P.; McFarlane, D.; Ali, R.; Dawes, W.; Barron, O.; Hodgson, G.; Charles, S. Groundwater Resource Assessment and Conceptualization in the Pilbara Region, Western Australia. *Earth Syst. Environ.* **2018**, *2*, 345–365. [CrossRef]
11. Renard, P.; Gómez-Hernández, J.J.; Schafmeister, M.T.; Varouchakis, E.A. Preface: Geostatistics and Hydrogeology. *Hydrogeol. J.* **2023**, *31*, 1383–1386. [CrossRef]
12. Tabari, H. Statistical Analysis and Stochastic Modelling of Hydrological Extremes. *Water* **2019**, *11*, 1861. [CrossRef]
13. Pool, M.; Carrera, J.; Alcolea, A.; Bocanegra, E.M. A Comparison of Deterministic and Stochastic Approaches for Regional Scale Inverse Modeling on the Mar Del Plata Aquifer. *J. Hydrol.* **2015**, *531*, 214–229. [CrossRef]

14. Rubin, Y.; Chang, C.F.; Chen, J.; Cucchi, K.; Harken, B.; Heße, F.; Savoy, H. Stochastic Hydrogeology's Biggest Hurdles Analyzed and Its Big Blind Spot. *Hydrol. Earth Syst. Sci.* **2018**, *22*, 5675–5695. [CrossRef]
15. Zhang, A.; Winterle, J.; Yang, C. Performance Comparison of Physical Process-Based and Data-Driven Models: A Case Study on the Edwards Aquifer, USA. *Hydrogeol. J.* **2020**, *28*, 2025–2037. [CrossRef]
16. Game, P.I. Hydrogeological Modeling for Real-Time Decision Support Systems Application to the Paillons Catchment. *France Ph.D. Thesis*; Côte d'Azur University, 2024. Polytech'Lab UPR. HAL, 241 pp. Available online: https://univ-cotedazur.hal.science/tel-04433795v1 (accessed on 20 April 2025).
17. Singh, A. Groundwater Resources Management through the Applications of Simulation Modeling: A Review. *Sci. Total Environ.* **2014**, *499*, 414–423. [CrossRef]
18. El Alfy, M. La Modélisation Numérique Des Écoulements Souterrains: Un Outil Efficace Pour La Gestion Des Ressources En Eau Dans Les Zones Arides. *Hydrol. Sci. J.* **2014**, *59*, 1259–1274. [CrossRef]
19. Moeck, C.; Affolter, A.; Radny, D.; Dressmann, H.; Auckenthaler, A.; Huggenberger, P.; Schirmer, M. Amélioration de La Gestion Des Ressources En Eau Pour Un Environnement Très Complexe En Utilisant Une Modélisation Tridimensionnelle Des Eaux Souterraines. *Hydrogeol. J.* **2018**, *26*, 133–146. [CrossRef]
20. Behera, A.K.; Pradhan, R.M.; Kumar, S.; Chakrapani, G.J.; Kumar, P. Assessment of Groundwater Flow Dynamics Using MODFLOW in Shallow Aquifer System of Mahanadi Delta (East Coast), India. *Water* **2022**, *14*, 611. [CrossRef]
21. Gurwin, J.; Lubczynski, M. Modeling of Complex Multi-Aquifer Systems for Groundwater Resources Evaluation—Swidnica Study Case (Poland). *Hydrogeol. J.* **2005**, *13*, 627–639. [CrossRef]
22. Smolyar, V.A.; Miroshnichenko, O.L.; Trushel, L.Y.; Sotnikov, E.V.; Mirlas, V.M. Structure of the Information System of Kazakhstan Fresh Groundwater Resources. *Ser. Geol. Tech. Sci.* **2022**, *4*, 182–198. [CrossRef]
23. Veselov, V. *Hydrogeological Zoning and Regional Assessment of Groundwater Resources in Kazakhstan*; Sydykov, Z., Ed.; Filim: Almaty, Kazakhstan, 2002.
24. Veselov, V.V.; Sydykov, Z.S. *Hydrogeology of Kazakhstan*; Sydykov, Z.S., Ed.; Ministry of Edication and Science of the Republic of Kazakhstan: Almaty, Kazakhstan, 2004.
25. Sapargaliyev, D.S.; Mirlas, V.M.; Murtazin, Y.Z.; Smolyar, V.A. Hydrogeological study and assessment of the groundwater resources in the cretaceous deposits of the Zhem basin. *Min. J. Kazakhstan* **2024**, *2*, 35–42.
26. Burakov, M.M.; Nedyuzhin, V.V.; Podolny, O.V. *Additional Exploration for the Purpose of Reassessing the Operational Reserves of Groundwater of the Kokzhide Field in the Aktobe Region, Completed in 2019–2021. with Calculation of Exploitable Reserves as of November 1, 2021*; KazGIDEK: Aktobe, Kazakhstan, 2021; 291p. (In Russian)
27. Zheksembaev, Y.M.; Nedyuzhin, V.V.; Podolny, O.V. *Additional Exploration for the Purpose of Re-Estimating Groundwater Reserves of the Kundaktykyrskoye, Bolshiye Barsuki and Ilekskoye Deposits in the Aktobe Region, Completed in 2012–2013. with Calculation of Exploitable Reserves as of 01.10.2013*; KazGIDEK: Aktobe, Kazakhstan, 2013; 254p. (In Russian)
28. Sapargaliyev, D.S.; Zheksembaev, Y.M.; Podolny, O.V. *Additional Exploration for the Purpose of Reassessing the Groundwater Reserves of the Kandagach, Embinsky-1 and Temir Deposits in the Aktobe Region Carried out in 2012–2013. with Calculation of the Murtazin Reserves as of 10/01/2013*; KazGIDEK: Aktobe, Kazakhstan, 2013; 342p. (In Russian)
29. Rachkov, S.I.; Burakov, M.M.; Podolny, O.V. *Additional Exploration for the Purpose of Reassessing the Exploitable Reserves of Groundwater of the Sarybulak Deposit in the Aktobe Region, Completed in 2020–2021 with the Calculation of Exploitable Reserves as of 12/01/2021*; KazGIDEK: Aktobe, Kazakhstan, 2021; 244p. (In Russian)
30. Murtazin, Y.Z.; Nurpeisov, R.A.; Sapargaliyev, D.S. *Additional Exploration for the Purpose of Reassessing the Exploitable Reserves of Groundwater of the Moiseevskoye Deposit in the Alginsky District of the Aktobe Region, Completed in 2020–2021 with the Calculation of Exploitable Reserves as of November 1, 2021*; Institute of Hydrogeology and Geo-ecology named after U.M. Akhmedsafin: Almaty, Republic of Kazakhstan, 2021; 139p. (In Russian)
31. Amon, E.O.; Blueford, J.R.; Wever, P.D.; Zhelezko, V.I. An Essay on Regional Geology and Stratigraphy of the Upper Cretaceous Deposits of Southern Urals Territories. *Geodiversitas* **1997**, *19*, 293–317.
32. Bear, J. *Hydraulics of Groundwater*; McGraw-Hill International Book Company: Mineola, NY, USA, 1979.
33. Schlumberger Water Services. *Visual MODFLOW 2011.1 User's Manual*; Schlumberger Water Services: Kitchener, ON, Canada, 2011.
34. Mirlas, V.; Kulagin, V.; Ismagulova, A.; Anker, Y. MODFLOW and HYDRUS Modeling of Groundwater Supply Prospect Assessment for Distant Pastures in the Aksu River Middle Reaches. *Sustainability* **2022**, *14*, 16783. [CrossRef]
35. Theis, C.V. The Relation between the Lowering of the Piezometric Surface and the Rate and Duration of Discharge of a Well Using Ground-water Storage. *Eos Trans. Am. Geophys. Union* **1935**, *16*, 519–524. [CrossRef]
36. Dierk Rhynsburger Analytic Delineation of Thiessen Polygons. *Geogr. Anal.* **1973**, *5*, 133–144. [CrossRef]
37. Anker, Y.; Gimburg, A.; Zilberbrand, M.; Livshitz, Y.; Mirlas, V. Groundwater Recharge Assessment for Small Karstic Catchment Basins with Different Extents of Anthropogenic Development. *Environments* **2023**, *10*, 158. [CrossRef]

38. Piper, A.M. A Graphic Procedure in the Geochemical Interpretation of Water-analyses. *Eos Trans. Am. Geophys. Union* **1944**, *25*, 914–928. [CrossRef]
39. Durov, S.A. Classification of natural waters and graphic presentation of their composition. *Dokl. Akad. Nauk* **1948**, *59*, 87–90.
40. Anker, Y. The Evolution of the Carbonate System in Hyper–Arid Environments (Central Arava Area, Israel), and Its Implication for 14C Groundwater Dating. Master's Thesis, The Hebrew University of Jerusalem, Jerusalem, Israel, 2003. Published as a Geological Survey of Israel report 2003. GSI/19/03, 109. (In Hebrew).
41. Anker, Y.; Flexer, A.; Rosenthal, E.; Ganor, E. Relationship between the Origin of Precipitation in the Jordan Rift Valley and Their Geochemical Composition. *J. Geophys. Res.* **2007**, *112*, 1–14. [CrossRef]
42. Mirlas, V.; Makyzhanova, A.; Kulagin, V.; Kuldeev, E.; Anker, Y. An Integrated Aquifer Management Approach for Aridification-Affected Agricultural Area, Shengeldy-Kazakhstan. *Water* **2021**, *13*, 2357. [CrossRef]
43. Mirlas, V.; Kulagin, V.; Ismagulova, A.; Anker, Y. Field Experimental Study on the Infiltration and Clogging Processes at Aksu Research Site, Kazakhstan. *Sustainability* **2022**, *14*, 15645. [CrossRef]
44. Smolyar, V.A.; Burov, B.V.; Mustafaev, S.T. *Water Resources of Kazakhstan: Assessment, Forecast, Management. Volume XIX. Groundwater in Kazakhstan: Availability and Use*; Institute of Geography: Almaty, Kazakhstan, 2012; pp. 36–52. (In Russian)
45. Muratkhanov, D.; Mirlas, V.; Anker, Y.; Miroshnichenko, O.; Smolyar, V.; Rakhimov, T.; Sotnikov, Y.; Rakhimova, V. Heavy Metal Groundwater Transport Mitigation from an Ore Enrichment Plant Tailing at Kazakhstan's Balkhash Lake. *Sustainability* **2024**, *16*, 6816. [CrossRef]

Disclaimer/Publisher's Note: The statements, opinions and data contained in all publications are solely those of the individual author(s) and contributor(s) and not of MDPI and/or the editor(s). MDPI and/or the editor(s) disclaim responsibility for any injury to people or property resulting from any ideas, methods, instructions or products referred to in the content.